RESEARCH ARTICLE

Comparative statistical analysis of the release kinetics models for nanoprecipitated drug delivery systems based on poly(lactic-co-glycolic acid)

Nathaly S. Heredia[ID][1☯], Karla Vizuete[ID][2☯]*, Marco Flores-Calero[3], Katherine Pazmiño V.[2], Fernanda Pilaquinga[ID][4], Brajesh Kumar[5], Alexis Debut[ID][1,2]

1 Departamento de Ciencias de la Vida y la Agricultura, Universidad de las Fuerzas Armadas ESPE, Sangolquí, Pichincha, Ecuador, **2** Centro de Nanociencia y Nanotecnología CENCINAT, Universidad de las Fuerzas Armadas ESPE, Sangolquí, Pichincha, Ecuador, **3** Departamento de Eléctrica, Electrónica y Telecomunicaciones, Universidad de las Fuerzas Armadas ESPE, Sangolquí, Pichincha, Ecuador, **4** Escuela de Ciencias Químicas, Pontificia Universidad Católica del Ecuador, Quito, Pichincha, Ecuador, **5** Department of Chemistry, TATA College, Chaibasa, Jharkhand, India

☯ These authors contributed equally to this work.
* ksvizuete@espe.edu.ec

Abstract

Poly(lactic-co-glycolic acid) is one of the most used polymers for drug delivery systems (DDSs). It shows excellent biocompatibility, biodegradability, and allows spatio-temporal control of the release of a drug by altering its chemistry. In spite of this, few formulations have reached the market. To characterize and optimize the drug release process, mathematical models offer a good alternative as they allow interpreting and predicting experimental findings, saving time and money. However, there is no general model that describes all types of drug release of polymeric DDSs. This study aims to perform a statistical comparison of several mathematical models commonly used in order to find which of them best describes the drug release profile from PLGA particles synthesized by nanoprecipitation method. For this purpose, 40 datasets extracted from scientific articles published since 2016 were collected. Each set was fitted by the models: order zero to fifth order polynomials, Korsmeyer-Peppas, Weibull and Hyperbolic Tangent Function. Some data sets had few observations that do not allow to apply statistic test, thus bootstrap resampling technique was performed. Statistic evidence showed that Hyperbolic Tangent Function model is the one that best fit most of the data.

Introduction

For more than 50 years, through nanotechnology and biomedicine, formulations and devices have been developed with the aim of improving the delivery and transport of drugs inside the human body [1–3]. The use of drug delivery systems (DDS) has brought great benefits such as altered drug pharmacokinetics, increased bioavailability, controlled and sustained drug

release, target therapy, combinatorial therapy, versatility in presentation modalities, simplified treatment schedules, suit clinical needs and patient preferences, decrease side effects, and increase patient treatment compliance [4–11]. DDS generally include: microsized forms as polymeric microspheres [12], microsponges [13], microneedles [14], and nanosized devices like liposomes [15], niosomes [16], metals nanoparticles [17], magnetic nanoparticles [18], nanocrystals [19], organic nanotubes [20], exosomes [21], and polymeric nanoparticles [22]. Especially, polymeric nanomaterials have attracted attention as DDS due to their excellent biocompatibility [23, 24] and biodegradability properties [25], as well as the *spatio-temporal* control of drug delivery [26]. Another attractive feature is that they allow the encapsulation of drugs with low water solubility and/or a short in vivo life, thus increasing their bioavailability over time [27].

One of the synthetic biodegradable polymers used in DDS is Poly (lactic-co-glycolic acid) or PLGA. This is a biopolymer synthesized from the polymerization of polyglycolic acid (PGA) and polylactic acid (PLA) monomers [28]. PLGA is stable, biocompatible, degradable under physiological conditions, non-immunogenic, and non-toxic, and commercially available with a wide range of different physicochemical properties [29]. The selection of specific characteristics such as its molecular weight, inherent viscosity or the LA:GA ratio allows to control the duration and behavior of the release profile of a PLGA DDS [28, 30–32]. These particularities make it suitable in applications such as tissue engineering [33], bioimaging [34], therapeutic devices, and pharmaceutical formulations as an excipient or as part of DDSs [35–37]. Therefore, several PLGA-based products are approved by the FDA and the European Medical Agency and are marketed to treat different conditions [28, 38, 39].

PLGA-based DDSs include morphologies such as microparticles or microspheres [40], nanofibers [41], films [42], foams [43], gels [44], nanoparticles [45, 46], among others [30, 35]. Being of a size that allows them to navigate freely through the body and remain for a long period of time in the blood circulatory system, nanoparticles, especially polymeric ones, have shown great potential as DDS [47, 48]. For instance, for long-term administration formulations, the time of permanence in blood varies between 24 hours (i.e. Lupron®, AbbVie Inc. [49]), 4 weeks (Lupron Depot®, AbbVie Inc. [50]), 12 weeks (Lupaneta Pack®, AbbVie Inc. [51]), to 24 weeks (i.e. Triptodur®, Arbor Pharmaceutics [52]). To optimally develop a drug delivery system, the release mechanisms and physicochemical processes involved in the transport and release of the active ingredient within an organism must be known, especially when working with nanometric systems. The main role of PLGA in these systems is the regulation of drug release kinetics in order to achieve a sustained and controlled release. This is made possible due to the ability to modify the biodegradability of the polymer by altering its chemistry (lactide/glycolide ratio), molecular weight, stoichiometry, functionalization of the terminal groups [53, 54], and by changing its size, shape, and porosity [55]. In addition, release disturbances caused by the particle's ability to absorb water and polymer-drug and drug-drug interactions may occur [30, 38, 56–58]. Drug transport systems made with PLGA nanoparticles tend to show a biphasic behavior in which initially there is a sudden release dominated by the diffusion phenomenon in which a high concentration of active agent is rapidly released in a short period of time [59], followed by a period of slow and continuous release, where polymer degradation/erosion is the most influential mechanism [60]. The initial stage is due to the presence of non-encapsulated drug molecules on the surface, drug particles attached to the surface of the nanoparticle [61], diffusion of the active compound through the polymeric matrix, diffusion of the encapsulated agent through water-filled pores, penetration of the surrounding medium from the surface to the center of the nanoparticle and activation of the hydrolytic degradation of the PLGA [58, 62]. Initial hydrolytic degradation of the polymer and diffusion of the drug through the polymer matrix are also present, although their impact is minor [30, 40,

58]. The hydrophilic or hydrophobic nature of the encapsulating agent and its molecular weight also play an important role in this phase [32]. This initial stage can be shortened or eliminated altogether by adjusting the nanoparticle synthesis technique [63]. The second phase is due to the integration of more complex mechanisms such as the existence of different crystalline and hydrated forms of the drug, the interactions formed between polymer and drug, and the plugging of solution-filled pores, which is the result of the formation of bonds between polymer chains [32, 64]. Sometimes a third and final phase is observed, in which the release increases because the degradation of the polymer within the nanoparticle is catalyzed by the decrease in pH generated by the acidic residues produced by the degradation of the nanoparticle surface. This phenomenon is known as autocatalytic heterogeneous degradation and is frequently observed in large particles [63].

Despite the benefits of using micro- and nanoformulations in drug delivery systems, not many products have reached the market [65]. This demonstrates the difficulty of developing PLGA encapsulations and consequently their high manufacturing cost, since at each stage of the design cycle, delivery methods need to be evaluated [66]. The development of advanced DDS depends on a carefully studied and monitored selection of the components. This can be facilitated by the use of mathematical models that allow predicting the rates and behavior of the drug release process, over-time drug concentration in the body, and the biological efficacy of developed DDSs [9, 67, 68]. By choosing the right model it would be possible to reduce the number of experiments required and gain an understanding of the physicochemical dynamic of the phenomena, thus facilitating the development of new pharmaceutical products [58, 69].

Mathematical models in general are able to interpret and predict experimental findings and are used as an abstraction of a real system with assumptions and simplifications [70]. These mathematical expressions provide a qualitative and quantitative description of the main phenomena involved in drug release by incorporating more parameters in their equation, related or not to physicochemical properties [71–73].

These models can be: i) mechanistic realistic: real phenomena such as drug diffusion or dissolution, erosion, swelling, precipitation, and degradation of the polymer are taken into account [74], so they can be complex to apply, or ii) empirical/semi-empirical: not based on real chemical, physical or biological phenomena but are partially realistic from the physical-chemical point of view and are therefore generally easy to apply and explain [75].

This study aims to perform a comparative statistical analysis of existing mathematical models of drug release kinetics from PLGA nanoparticle-based DDSs engineered by nanoprecipitation to find which one could be the most suitable general model for describing the release profile.

Materials and methods

Forty data sets describing the over-time drug release of different PLGA nanoformulations as synthesized using nanoprecipitation techniques were extracted from twenty scientific articles. The articles were selected by searching for the following keywords or combinations: "drug release systems", "poly(lactic-co-glycolic acid)", "PLGA", "nanoprecipitation" in academic search engines such as Google Scholar, PubMed y NCBI. To limit the study, the authors selected scientific articles from 2016. Furthermore, to the best of our knowledge, this was the year in which the mathematical model of hyperbolic tangent function was applied for the first time to evaluate the release profile of core-shell lipid nanoparticles [76]. From each data set, the characteristics of the nanoparticle such as encapsulated drug, size, shape, and surface modifications, as well as the characteristics of the polymer used such as LA/GA ratio and molecular weight or inherent viscosity, among others, were listed. Fig 1 illustrates the search process for
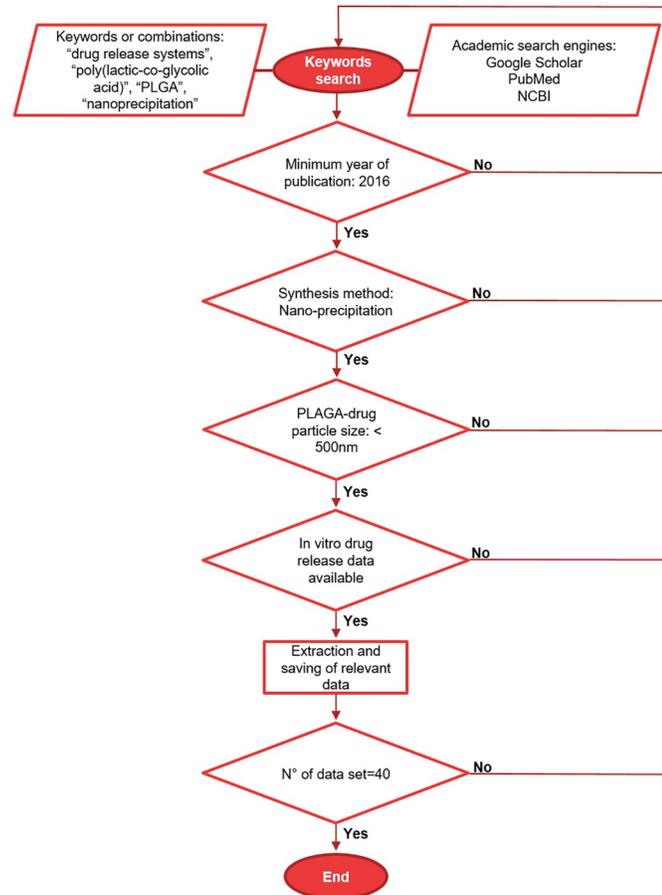
Fig 1. Flow diagram for the screening procedure and selection criteria for the scientific articles chosen in this study.

https://doi.org/10.1371/journal.pone.0264825.g001

the scientific articles selected for this study. The data sets obtained can be found in the supplementary information.

Forty data sets obtained were fitted by linear sum-of-squares regression to five conventional empirical/semi-empirical models:

Zero-order: The release kinetics of an agent is only a function of time, and the process takes place at a constant rate independent of the concentration of the active agent [77].

$$Q_t = k_0 \times t + Q_0 \tag{1}$$

Where:

Q_t = percentage of the released drug after time t.

Q_0 = initial percentage of the released drug (Usually 0).

k_0 = rate constant for zero-order kinetics.

t = time.

First-order: First-order release kinetics states that the variation in concentration with respect to time depends only on the concentration of the active agent remaining in the

device [78].

$$\ln(Q_t) = \ln(Q_o) + k_1 \qquad (2)$$

Where:

Q_t = percentage of the released drug after time t.

Q_0 = initial percentage of the released drug (Usually 0).

k_1 = rate constant for first-order kinetics.

t = time.

Korsmeyer-Peppas: It is used to describe drug release from a polymeric system considering non-fickian mechanisms [79]. The model is useful when the release mechanism is unknown or when more than one type of drug release phenomenon is involved [77, 80]. Even if Peppas (1985) points out that this model is applicable only for the first 60% of the release curve; however, we analyzed it in both cases, 60% and 100% drug release profile [81].

$$\ln(Q_t) = \ln(k_{KP}) + n \ln(t) \qquad (3)$$

Where:

Q_t = percentage of the released drug after time t.

k_{KP} = constant of nanoparticles incorporating geometric characteristic structures.

n = release exponent (related to the drug release mechanism).

t = time.

Weibull: It is an empirical model that serves as a theoretical basis for almost all release kinetics in heterogeneous matrices. It represents a distribution function describing a phenomenon associated with a finite time [40, 80].

$$\ln[-\ln(1 - Q_t)] = \ln(\propto) + \beta \cdot \ln(t) \qquad (4)$$

Where:

Q_t = percentage of the released drug after time t.

α = scale parameter, defines the timescale of the process.

β = curve shape factor.

t = time.

Hyperbolic tangent function: This function arises from the modification of the diffusive release model used by Korsmeyer-Peppas with the intention of being able to extend the mathematical expression to the entire release curve of a homogeneous particle [73, 76].

$$\mathrm{atanh}(Q_t/Q_\infty) = \propto t^{\frac{1}{2}} + \beta \qquad (5)$$

Where:

Q_∞ = total percentage of the released drug.

Q_t = percentage of the released drug after time t.

α = constant related to particular size and diffusion constant.

Fig 2 shows a time-line of the development of the mathematical models used in this study.

In addition, the 40 data sets were fitted by regression to second to fifth order polynomials, according to the equations shown in S1 File.

The fitting process of each model was carried out by means of simple linear regression analysis by sum of squares in the free software R [87]. Model acceptance criteria, such as the linear regression indexes (intercept I and slope S), regression coefficient (R^2), adjusted or corrected regression coefficient (R^2_a), sum of squares of residual (SSR), sum of squares of the error (SSE), sum square of total variation (SST), the T-statistic and the F-statistic were calculated using the function "lm" in R [88].
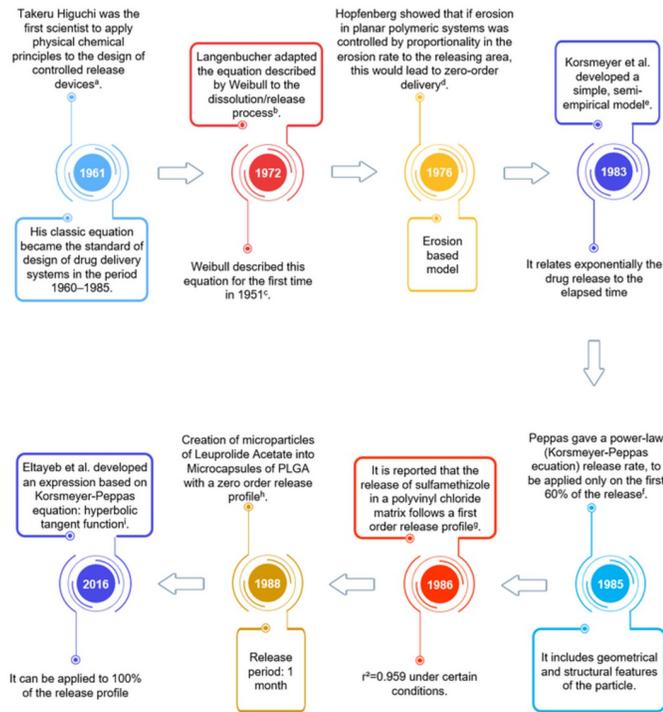
Fig 2. Time-line of conventional empirical/semi-empirical models. a. [82]; b. [83]; c. [84]; d. [85]; e. [79]; f. [81]; g. [86]; h. [50]; i. [76].

The significance test of the t-statistic (t-value) was used to evaluate the capacity of the parameters to linearly relate the dependent variable to the independent variable. In this test the following hypotheses were considered:

$$\text{Null hypothesis } H_0 : \beta_i = 0$$

$$\text{Alternative hypothesis } H_a : \beta_i \neq 0$$

Considering β_i as the *i-th* analyzed parameter. Following the rejection rule, for a significance level of $\propto = 0.05$, in a two-tailed test, the critical value according to the probability table is $|t| > 1.96$, therefore:

$$\text{Reject } H_0 \text{ if } |t| \geq 1.96$$

$$\text{Reject } H_0 \text{ if } p - valor \leq 0.05$$

By rejecting H_0, it is concluded that $\beta_i \neq 0$ and hence a statistically significant relationship between the variables analyzed [89].

In case of the intercept, when the null hypothesis was accepted by means of the critical value or the p-value, it was recalculated considering the intercept as 0. If the null hypothesis is accepted for the slope, then the model was rejected.

On the other hand, the significance test of F-statistic, like t-statistic, indicates whether there is a significant relationship between the independent and dependent variables. In this sense, if only one parameter is analyzed, it will lead to the same conclusion as the t-statistic, but, having

more parameters, F-test can prove that there is an overall significant relationship. In this case, same hypotheses were assumed:

$$H_0 : \beta_i = 0$$

$$H_a : \beta_i \neq 0$$

The rejection criteria were:

$$\textit{Reject } H_0 \textit{ if } F \geq F_\propto$$

$$\textit{Reject } H_0 \textit{ if } p - value \leq 0.05$$

By rejecting H_0, it is concluded that there is a statistically significant relationship between the analyzed variables [89], conversely, if $p - value > 0.05$ the model was rejected.

Additionally, using the R function *"glance"* of the package *"broom"* the value of the Akaike Information Criterion (AIC) and Bayesian Information Criterion (BIC) were calculated for each of the fits [90].

The equations for the mathematical model acceptance criteria are summarized in S1 File.

Whereas the data sets obtained from literature contain few cumulative percentage values over time (3–14 per set), Bootstrap resampling technique was employed. This is a resampling method for statistical inference when the original sample is small. The technique seeks to create multiple data subsets from a real data set without making arbitrary assumptions, with the new data set being equally representative of the target population [91]. It is also commonly used to estimate confidence intervals, bias, and variance of an estimator or to calibrate hypothesis tests [92], see Fig 3.

In this study, the Bootstrap resampling technique was used to estimate the values of intercept, slope, and R^2 with 1000 Bootstrap samples using the "Boot" function. This requires the packages: "carData" [93], "car" [94], and "MUMIn" [95]. To correct the AIC value, we applied the function "boot.stepAIC" of the libraries "bootStepAIC" [96] and "MASS" [97]. In addition, the confidence interval for each of the parameters corrected to 95% was calculated with the function "confint" (S3 File).
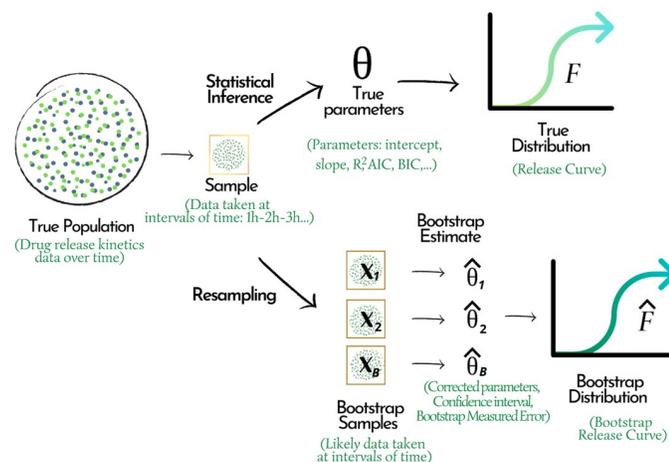

Fig 3. Diagram of the process for parameter estimation by Bootstrap resampling.

https://doi.org/10.1371/journal.pone.0264825.g003

Results

The cumulative drug release data extracted from the scientific articles collected are described in detail with the data in S2 File. Also, Table 1 briefly describes the polymer used for the synthesis, the drug encapsulated, the main characteristics of the nanoparticles obtained, the parameters under which the release assay was performed (release medium and duration) and the percentage of drug release achieved in each case. It can be observed that in 80% of the tests carried out, PLGA with an L/G ratio of 50:50 was used, being the polymer with a molecular weight of 7–17 kD the most commonly used. One hundred percent of the nanoparticles generated are nearly spherical and have a size range between 60 and 550 nm, and only 25% of the formulations performed surface modifications. On the other hand, the drug release conditions were variable. 32 of the release assays were performed in Phosphate buffer saline (PBS), 3 in hydrochloric acid, 2 in Phosphate buffer (PB), 2 in Fetal bovine serum (FBS) and 1 in Simulated body fluids (STF). The time to study drug release ranged from 3 hours to 21 days (504 hours). Finally, the number of observations per set was also variable. 20% of the data presented 6 observations, 17.5% 8 observations, 15% 14 observations, 12.5% 7 observations, 10% 5 observations, another 10% 9 observations, 5% 3 observations and only one data set presented 4, 10, 11 and 12 observations respectively.

S3 File shows, by means of an example using set number 33 [111] and its fit to the Korsmeyer-Peppas model, the program used to fit the mathematical models in the statistical program R.

S4 File shows the results of the fit and the acceptance criteria for each studied mathematical model and polynomial. The first criteria for rejecting a mathematical model was to evaluate the slope and F-statistic, after recalculating with intercept = 0 if necessary. Table 2 shows the results obtained. In the case of zero-order fit, sets 7–10, 18 and 19 were rejected, for first-order sets 5–11, 18, 19, 28, 29, 34 and 40, for Korsmeyer-Peppas 100% sets 7–9, 18 and 19, for Korsmeyer-Peppas 60% sets 7–10, 18, 26, 27, 28 and 36, for Weibull sets 7–9 and 18, and for Hyperbolic Tangent only the fit for sets 7 to 9 was rejected. It is important to note that no model was adequately fit for sets 7, 8 and 9. In some cases the number of observations limited the application of the statistical analysis in R. Specifically for the Korsmeyer-Peppas 60% model, it was not possible to perform the analysis on sets 7–10, 18, 26, 26, 27 and 36 because with the two first observations the set exceeded 60% of the release curve. We analyzed R^2- R^2_a values, and AIC-BIC of previously un-rejected models. The best fit for each dataset is detailed in Table 3. According to these criteria, none of the datasets fit the zero-order and first-order models. Neither model fitted Weibull according to AIC and BIC. When studying in parallel R^2- R^2_a and AIC-BIC only 48% of the sets accept the same model under these two criteria, which indicates that they are not equivalent. The mathematical model with the largest number of data sets with adequate fit is the hyperbolic tangent. Following R^2- R^2_a and AIC-BIC criteria, 48% and 65% of the sets fit this model best, respectively. In addition, sets 7, 8 and 9 sets (8% of the data) did not fit any model.

Regarding the fit to the polynomial equations, the value of the intercept was analyzed (*a* letter in all polynomial functions) following the criteria mentioned in the methodology section. If null hypothesis was accepted, then the statistics were recalculated with a value of intercept = 0. If the value of the last term, represented by the letters *c*, *d*, *e*, *f* for each polynomial degree respectively, was equal to zero the model was rejected since the equation is transformed into one of a lower degree. The results are described in Table 4. Through this analysis it was found that in this particular case, the results obtained by AIC-BIC y R^2—R^2_a are the same for all sets. Nine of the forty datasets did not fit any model. In accordance with the t-value and p-value of the last term, 11 data sets were rejected for the second-degree equation, 23 for the

Table 1. Main characteristics of the 40 datasets analyzed.

No	Drug	Polymer	Lactide: Glycolide ratio	MW [kDa] or Inherent viscosity [dL g^{-1}]	NP shape	NP size [nm]	Surface modification	Release medium	Time range [hours]	Total Release percentage [%]	Year	Ref.
1	Paclitaxel	PLGA	(50:50)	NM	Spherical	166.9±5.0	-	PBS	168	80	2016	[98]
2	Paclitaxel	PLGA-Tween 80	(50:50)	NM	Spherical	156.5±8.6	-	PBS	168	75	2016	[98]
3	Simvastatin	PLGA	(50:50)	0.2 dL g^{-1}	Spherical	99–129	TPGS Liposome	PBS	240	68	2018	[99]
4	Ketamine	PLGA-PEG	(50:50)	5–55 kDa	Spherical	98.8±0.9	-	PBS	504	82	2020	[100]
5	Ketamine	PLGA-PEG	(50:50)	5–55 kDa	Spherical	80–300	Shellac	PBS	504	58	2020	[100]
6	Carbamazepine	PLGA	(50:50)	7–17 kDa	Spherical	180.6±6.2	-	PB	48	90	2020	[101]
7	Levetiracetam	PLGA	(50:50)	7–17 kDa	Spherical	180.6±6.2	-	PB	48	100	2020	[101]
8	Ibuprofen	PLGA-PVA	(50:50)	24–38 kDa	Spherical	100–200	-	PBS	3	100	2017	[102]
9	Ibuprofen	PLGA-PVA	(50:50)	24–38 kDa	Spherical	100–200	-	PBS	3	100	2017	[102]
10	Dil	PLGA	(50:50)	24–38 kDa	Spherical	157.9±6.1	-	PBS	24	88	2017	[103]
11	Dil	PLGA	(50:50)	24–38 kDa	Spherical	230.8±4.3	-	PBS	24	79	2017	[103]
12	N-acetilcysteine	PLGA	(75:25)	25–90 kDa	Spherical	145–205	-	PBS	168	100	2018	[104]
13	Dexamethasone	PLGA-PEG	(50:50)	5 kDa	Spherical	250–400	-	PBS	360	60	2017	[105]
14	Paclitaxel	PLGA	(50:50)	1–50 kDa	Spherical	140±5	-	PBS	240	86	2017	[106]
15	Paclitaxel	PLGA	(75:25)	NM	Spherical	120±5	-	PBS	240	88.5	2017	[106]
16	Paclitaxel	PLGA	(50:50)	1–50 kDa	Spherical	140±5	-	PBS	240	87.5	2017	[106]
17	Paclitaxel	PLGA	(75:25)	128 kDa	Spherical	120±5	-	PBS	240	89	2017	[106]
18	Paclitaxel	PLGA	(50:50)	NM	Spherical	60–450	-	FBS	3	100	2017	[107]
19	Sorafenib	PLGA	(50:50)	NM	Spherical	70–550	-	FBS	3	100	2017	[107]
20	Ropinirole HCl	PLGA-PVA	(50:50)	NM	Spherical	308.3±23	Polysorbate 80	PBS	24	42	2020	[108]
21	Ropinirole HCl	PLGA-PVA	(50:50)	NM	Spherical	345.5±42	Polysorbate 80	PBS	24	36	2020	[108]
22	Ropinirole HCl	PLGA-PVA	(50:50)	NM	Spherical	264.6±11	Polysorbate 80	PBS	24	43	2020	[108]
23	Ropinirole HCl	PLGA-PVA	(50:50)	NM	Spherical	212±3	Polysorbate 80	PBS	24	58	2020	[108]
24	Ropinirole HCl	PLGA-PVA	(50:50)	NM	Spherical	351.9±20	Polysorbate 80	PBS	24	44	2020	[108]
25	Ropinirole HCl	PLGA-PVA	(50:50)	NM	Spherical	196.4±8	Polysorbate 80	PBS	24	62	2020	[108]
26	Ciprofloxacin	PLGA-PEG	(50:50)	30–35 kDa	Spherical	174–205	-	STF	144	95	2019	[109]
27	Methotrexate	PLGA-PVA	(50:50)	7–17 kDa	Spherical	78.1±7.3	-	PBS	72	92	2019	[46]
28	Methotrexate & Curcumin	PLGA-PVA	(50:50)	7–17 kDa	Spherical	148.3±4.1	-	PBS	72	80	2019	[46]
29	Curcumin	PLGA-PVA	(50:50)	7–17 kDa	Spherical	92.4±5.2	-	PBS	72	75	2019	[46]
30	Methotrexate & Curcumin	PLGA-PVA	(50:50)	7–17 kDa	Spherical	148.3±4.1	-	PBS	72	57	2019	[46]
31	Curcumin	PLGA	(75:25)	65 kDa	Spherical	280±16	-	PBS	120	68	2018	[110]
32	Curcumin	PLGA	(75:25)	65kDa	Spherical	251±3	Anti-EGFRvIII antibodies	PBS	120	69	2018	[110]
33	MTPC	PLGA-PEG	(50:50)	17 kDa	Spherical	143.2±3.7	-	PBS	4	62	2020	[111]
34	Lansoprazole	PLGA	(50:50)	NM	Spherical	246.7±3.4	-	PBS	48	92	2019	[112]
35	Saquinavir	PLGA	(50:50)	NM	Spherical	412.2	-	PBS	16	99	2020	[113]
36	Insulin	PLGA-PEG	(50:50)	10 kDa	Spherical	78.7	Zinc chloride	PBS	8	100	2017	[37]
37	Paclitaxel	PLGA-PEG	(50:50)	55 kDa	Spherical	100	-	PBS	168	39	2020	[114]
38	Olmesartan medoxomil	PLGA	(75:25)	4–15 kDa	Spherical	71.2±4.5	-	HCl	24	39	2016	[45]
39	Olmesartan medoxomil	PLGA	(75:25)	4–15 kDa	Spherical	78.9±3.2	-	HCl	24	30	2016	[45]

(Continued)

Table 1. (Continued)

No	Drug	Polymer	Lactide: Glycolide ratio	MW [kDa] or Inherent viscosity [dL g^{-1}]	NP shape	NP size [nm]	Surface modification	Release medium	Time range [hours]	Total Release percentage [%]	Year	Ref.
40	Olmesartan medoxomil	PLGA	(75:25)	4–15 kDa	Spherical	97.8±6.3	-	HCl	24	35	2016	[45]

Notation: MW: molecular weight, NM: Not mentioned in the source, "-": Not applicable, PLGA: poly (lactic-co-glycolic acid), PVA: polyvinyl alcohol; PEG: polyethylene glycol, TPGS; Dil: 1,10-dioctadecyl-3,3,30,30-tetramethylindocarbocyanine perchlorate, MTPC: N′-(2-Methoxybenzylidene)-3-methyl-1-phenyl-H-Thieno [2,3-c]Pyrazole-5-arbohyd-razide, PBS: Phosphate buffer saline, PB: Phosphate buffer, STF: Simulated body fluids, FBS: Fetal bovine serum, HCl: hydrochloric acid.

https://doi.org/10.1371/journal.pone.0264825.t001

third-order equation, 27 for the fourth-order equation, and 25 for the fifth-order equation. AIC-BIC and R^2—R^2_a showed that the polynomial equation that provided the best fit to the largest amount of data was the second-degree equation (38%), followed by the third-degree equation (20%), the fifth-degree equation (13%) and finally the fourth-degree equation (8%). It is worth noting that when the average R^2—R^2_a of the data sets unrejected previously were evaluated, it was found that these values tend to increase as the degree of the polynomial increases, as can be seen in Fig 4.

Moreover, when Bootstrap resampling was performed (S5 File) it could be found that the best fit for data sets 7, 8 and 9 is Korsmeyer-Peppas 100% or zero-order by R^2 and Korsmeyer-Peppas 100% by AIC, see Table 5. More specifically, by AIC, 30% of the sets present a better fit with Korsmeyer-Peppas 100% and 70% with Hyperbolic Tangent for polynomial equations 13%, 23%, 23%, 23%, and 33% were fit to second to fifth degree polynomials respectively. In addition, a single data set fitted to all polynomials and 3 to none. It is important to note that by analyzing the coefficient of determination of the resampled data, more than one model is accepted. As the best fit, by using the AIC with the most negative value, the model or polynomial equation that best fits the data can be determined.

Finally, Figs 5–7 show scatter diagrams of R^2 in relation to AIC and BIC for the models analyzed, both for the values obtained by linear regression and the Bootstrap corrected values. Additionally, the region of what is considered a good fit is indicated: between 0.8 and 1 for R^2 and between 0 and -inf for AIC and BIC. In both figures it can be clearly observed how in the Hyperbolic Tangent Function model the data sets are mostly grouped in the region considered as having the best fit.

Discussion

In this study, five general controlled drug release models and four polynomial equations, from the second to the fifth degree, were statistically analyzed. The main objective was to find a mathematical expression that can describe the release mechanism of an active compound observed in PLGA nanoparticles synthesized by nanoprecipitation method.

While it is true that mathematical models are tools that help to understand the dynamics of a drug release, and to save time and money [115], it is important to note that these also have shortcomings in terms of predictive power and in explaining and addressing all the physical, chemical and biological phenomena involved since they mainly describe the dominant event [62]. Among them is the initial burst release, as the fraction released can sometimes approach 80% of the total encapsulated agent [116] in a time that may be less than 10% of the duration of the entire release process [48, 52]. In addition, very few models described in the literature

Table 2. Evaluation of the p-value of the intercept, slope and F-statistic of the datasets.

Model is rejected if:	Zero order			First order			Korsmeyer Peppas 100%			Korsmeyer Peppas 60%			Weibull			Hyperbolic Tangent		
	$\|t\|<1{,}96$ $p>0{,}05$ I	$\|t\|<1{,}96$ $p>0{,}05$ S	$p>0{,}05$ Est F	$\|t\|<1{,}96$ $p>0{,}05$ I	$\|t\|<1{,}96$ $p>0{,}05$ S	$p>0{,}05$ Est F	$\|t\|<1{,}96$ $p>0{,}05$ I	$\|t\|<1{,}96$ $p>0{,}05$ S	$p>0{,}05$ Est F	$\|t\|<1{,}96$ $p>0{,}05$ I	$\|t\|<1{,}96$ $p>0{,}05$ S	$p>0{,}05$ Est F	$\|t\|<1{,}96$ $p>0{,}05$ I	$\|t\|<1{,}96$ $p>0{,}05$ S	$p>0{,}05$ Est F	$\|t\|<1{,}96$ $p>0{,}05$ I	$\|t\|<1{,}96$ $p>0{,}05$ S	$p>0{,}05$ Est F
1	A	A	A	A	X	X	A	A	A	A	A	A	A	A	A	A	A	A
2	A	A	A	A	X	X	A	A	A	A	A	A	A	A	A	A	A	A
3	A	A	A	A	A	A	A	A	A	A	A	A	A	A	A	A	A	A
4	A	A	A	A	A	A	A	A	A	RC	A	A	A	A	A	A	A	A
5	A	A	A	A	X	X	RC	A	A	RC	A	A	A	A	A	RC	A	A
6	A	A	A	A	X	X	A	A	A	A	A	A	A	A	A	RC	A	A
7	A	X	X	RC	X	X	A	X	X	Insufficient data	Insufficient data	Insufficient data	Insufficient data	Insufficient data	Insufficient data	Insufficient data	Insufficient data	Insufficient data
8	RC	X	X	RC	X	X	A	X	X	Insufficient data	Insufficient data	Insufficient data	Insufficient data	Insufficient data	Insufficient data	Insufficient data	Insufficient data	Insufficient data
9	RC	X	A	A	X	X	A	X	X	Insufficient data	Insufficient data	Insufficient data	Insufficient data	Insufficient data	Insufficient data	Insufficient data	Insufficient data	Insufficient data
10	RC	A	X	A	X	X	A	A	A	Insufficient data	Insufficient data	Insufficient data	A	A	A	RC	A	A
11	RC			A	X	X	A	A	A	Insufficient data	Insufficient data	Insufficient data	A	RC	A	A	A	A
12	A	A	A	A	A	A	A	A	A	A	A	A	A	A	A	A	A	A
13	A	A	A	A	A	A	A	A	A	A	A	A	A	A	A	A	A	A
14	A	A	A	A	A	A	A	A	A	A	A	A	A	A	A	A	A	A
15	A	A	A	A	X	X	X	X	X	A	X	A	A	A	A	A	A	A
16	A	A	A	A	A	A	A	A	A	X	A	X	A	A	A	A	A	A
17	A	A	A	A	A	A	A	A	A	A	A	A	A	A	A	A	A	A
18	RC	X	X	A	X	X	A	X	X	RC	A	A	RC	X	X	RC	A	A
19	RC	X	X	A	X	X	A	X	X	A	RC	A	RC	A	A	A	A	A
20	A	A	A	A	A	A	A	A	A	A	A	A	RC	A	A	A	A	A
21	A	A	A	A	A	A	A	A	A	A	A	A	A	A	A	A	A	A
22	A	A	A	A	A	A	A	A	A	A	A	A	A	A	A	A	A	A
23	A	A	A	A	A	A	A	A	A	A	A	A	A	A	A	A	A	A
24	A	A	A	A	A	A	A	A	A	X	X	X	A	A	A	A	A	A
25	A	A	A	A	A	A	A	A	A	A	A	A	A	A	A	A	A	A
26	A	A	A	A	A	A	A	A	A	Insufficient data	Insufficient data	Insufficient data	A	A	A	A	A	A
27	A	A	A	A	A	A	A	A	A	Insufficient data	Insufficient data	Insufficient data	A	A	A	A	A	A
28	A	A	A	A	X	X	A	A	A	A	X	X	A	A	A	A	A	A
29	A	A	A	A	X	X	A	A	A	A	A	A	A	A	A	A	A	A
30	A	A	A	A	A	A	A	A	A	A	A	A	A	A	A	A	A	A
31	A	A	A	A	A	A	A	A	A	A	A	A	A	A	A	A	A	A
32	A	A	A	A	A	A	A	A	A	A	A	A	A	A	A	A	A	A
33	RC	A	A	A	A	A	A	A	A	A	A	A	A	A	A	A	A	A
34	A	A	A	A	A	X	A	A	A	A	A	A	A	A	A	A	A	A
35	A	A	A	A	A	A	A	A	A	A	A	A	A	A	A	A	A	A

(*Continued*)

Table 2. (Continued)

Model is rejected if:	Zero order			First order			Korsmeyer Peppas 100%			Korsmeyer Peppas 60%			Weibull			Hyperbolic Tangent		
	I ($|t|<1,96$, $p>0,05$)	S ($|t|<1,96$, $p>0,05$)	Est F ($p>0,05$)	I ($|t|<1,96$, $p>0,05$)	S ($|t|<1,96$, $p>0,05$)	Est F ($p>0,05$)	I ($|t|<1,96$, $p>0,05$)	S ($|t|<1,96$, $p>0,05$)	Est F ($p>0,05$)	I ($|t|<1,96$, $p>0,05$)	S ($|t|<1,96$, $p>0,05$)	Est F ($p>0,05$)	I ($|t|<1,96$, $p>0,05$)	S ($|t|<1,96$, $p>0,05$)	Est F ($p>0,05$)	I ($|t|<1,96$, $p>0,05$)	S ($|t|<1,96$, $p>0,05$)	Est F ($p>0,05$)
36	A	A	A	A	A	A	A	A	A	Insufficient data			A	A	A	A	A	A
37	A	A	A	A	A	A	A	A	A			A	A	A	A	A	A	A
38	RC	A	A	A	A	A	A	A	A	A	A	A	A	A	A	A	A	A
39	RC	A	A	A	A	A	A	A	A	A	A	A	A	A	A	A	A	A
40	RC	A	A	A	A	X	A	A	A	A	A	A	A	A	A	A	A	A

Notation: "I": Intercept; "S": Slope "RC": Recalculated; "A": Accepted model; "X": Rejected model.

https://doi.org/10.1371/journal.pone.0264825.t002

Table 3. Best fit for each data set according to R^2, R^2_a, AIC and BIC.

No.	R^2—R^2_a	AIC—BIC	No.	R^2—R^2_a	AIC—BIC
1	Korsmeyer-Peppas 60%	Korsmeyer-Peppas 60%	21	Hyperbolic Tangent	Hyperbolic Tangent
2	Korsmeyer-Peppas 60%	Hyperbolic Tangent	22	Hyperbolic Tangent	Hyperbolic Tangent
3	Weibull	Hyperbolic Tangent	23	Hyperbolic Tangent	Hyperbolic Tangent
4	Hyperbolic Tangent	Hyperbolic Tangent	24	Weibull	Hyperbolic Tangent
5	Hyperbolic Tangent	Hyperbolic Tangent	25	Hyperbolic Tangent	Hyperbolic Tangent
6	Hyperbolic Tangent	Hyperbolic Tangent	26	Hyperbolic Tangent	Korsmeyer-Peppas 100%
7	No model	No model	27	Weibull	Korsmeyer-Peppas 100%
8	No model	No model	28	Hyperbolic Tangent	Hyperbolic Tangent
9	No model	No model	29	Weibull	Hyperbolic Tangent
10	Hyperbolic Tangent	Hyperbolic Tangent	30	Weibull	Hyperbolic Tangent
11	Hyperbolic Tangent	Hyperbolic Tangent	31	Weibull	Hyperbolic Tangent
12	Weibull	Hyperbolic Tangent	32	Weibull	Hyperbolic Tangent
13	Weibull	Hyperbolic Tangent	33	Hyperbolic Tangent	Hyperbolic Tangent
14	Weibull	Hyperbolic Tangent	34	Korsmeyer-Peppas 60%	Korsmeyer-Peppas 60%
15	Weibull	Korsmeyer-Peppas 100%	35	Korsmeyer-Peppas 60%	Korsmeyer-Peppas 100%
16	Korsmeyer-Peppas 60%	Korsmeyer-Peppas 100%	36	Weibull	Korsmeyer-Peppas 100%
17	Korsmeyer-Peppas 60%	Korsmeyer-Peppas 60%	37	Hyperbolic Tangent	Hyperbolic Tangent
18	Hyperbolic Tangent	Hyperbolic Tangent	38	Hyperbolic Tangent	Hyperbolic Tangent
19	Korsmeyer-Peppas 60%	Korsmeyer-Peppas 60%	39	Hyperbolic Tangent	Hyperbolic Tangent
20	Hyperbolic Tangent	Hyperbolic Tangent	40	Hyperbolic Tangent	Hyperbolic Tangent

consider the effect of drug properties, especially acids, on the degradation rate of polymer particles [117]. It should not be forgotten that mathematical models are approximations of reality where assumptions are made, so they should always be accompanied by experimental data that can support these assertions [118–120]. Empirical and semi-empirical mathematical models tend to have limited predictive power, so it is recommended that these theories be applied, and be of great use, when you want to compare release profiles using a specific parameter [121].

On the other hand, the coefficient of determination "R^2" is one of the most widely used criteria to determine whether or not a model is a better fit to a release curve. However, it has been widely demonstrated that R^2 can increase, i.e., tends more to one, if more variables are added to the equation, even if they are completely irrelevant to the model [122]. This problem is more accentuated when the number of observations is insufficient [123]. Similarly, R^2 is not considered an appropriate goodness-of-fit criterion when analyzing multi-parameter models, as our study. Therefore, taking into account the adjusted coefficient of determination R^2_a is the most appropriate, although in a limited way, since its value only increases when a relevant variable is added to the model, otherwise it decreases [124]. Since there is no perfect correlation between the variables, special care should be taken in the interpretation of the results when R^2 or R^2_a take the value of 1 [125]. In addition, it is recommended to accompany these criteria with statistical procedures such as t-test, F-test, and prediction intervals to know the quality and influence of individual observations in the estimation [126].

Since the Bayesian and Akaike criteria are based on the addition of statistical errors corrected by a penalty function proportional to the number of parameters, they can be a good alternative to determine which model offers the best fit. In addition, these criteria help to determine whether the inclusion of a term, or increased complexity in the equation, results in better fit [127]. It is important to emphasize that models with more negative values of AIC and

Table 4. Evaluation of the p-value of the intercept, last term, and F-statistic of the data sets.

Model is rejected if:	2nd order			3rd order			4th order			5th order		
	$\lvert t \rvert < 1{,}96$ p>0,05 a	$\lvert t \rvert < 1{,}96$ p>0,05 LT	p>0,05 Est F	$\lvert t \rvert < 1{,}96$ p>0,05 a	$\lvert t \rvert < 1{,}96$ p>0,05 LT	p>0,05 Est F	$\lvert t \rvert < 1{,}96$ p>0,05 a	$\lvert t \rvert < 1{,}96$ p>0,05 LT	p>0,05 Est F	$\lvert t \rvert < 1{,}96$ p>0,05 a	$\lvert t \rvert < 1{,}96$ p>0,05 LT	p>0,05 Est F
1	A	X	-	A	X	-	A	X	-	RC	A	A
2	A	X	-	A	X	-	A	X	-	A	X	-
3	A	A	A	A	A	A	A	A	A	A	A	A
4	RC	A	A	RC	X	-	Insufficient data			Insufficient data		
5	RC	A	A	RC	X	-						
6	A	A	A	RC	X	-	RC	X	-	RC	X	-
7	Insufficient data			Insufficient data			Insufficient data			Insufficient data		
8												
9												
10	RC	A	A	A	A	A						
11	RC	A	A	RC	X	-						
12	A	X	-	A	X	-	A	X	-	A	X	-
13	A	A	A	A	A	A	A	X	-	A	X	-
14	A	A	A	A	A	A	A	X	-	A	X	-
15	A	A	A	A	X	-	A	X	-	A	X	-
16	A	A	A	A	A	A	A	X	-	A	A	A
17	A	A	A	A	X	-	A	A	A	A	X	-
18	RC	A	A	RC	X	-	RC	X	X	Insufficient data		
19	RC	A	A	A	A	A	A	X	-	RC	A	A
20	A	A	A	A	A	A	A	X	-	A	X	-
21	A	A	A	A	A	A	A	X	-	A	X	-
22	A	A	A	A	X	-	A	X	-	A	A	A
23	A	A	A	A	X	-	A	X	-	A	X	-
24	A	A	A	A	X	-	A	X	-	A	X	-
25	A	A	A	A	X	-	A	X	-	A	X	-
26	A	X	-	A	A	A	A	A	A	A	X	-
27	A	X	X	A	X	X	A	X	X	Insufficient data		
28	A	X	-	A	A	A	RC	X	-			
29	A	X	-	RC	X	-	RC	A	A			
30	A	X	-	A	A	A	A	X	-			
31	A	A	A	A	X	-	A	X	-	A	X	-
32	A	A	A	A	X	-	A	X	-	A	X	-
33	RC	X	-	RC	X	-	RC	X	-	Insufficient data		
34	A	A	A	A	A	A	RC	A	A	RC	X	-
35	A	A	A	A	X	-	A	X	-	RC	X	-
36	RC	A	A	RC	A	A	RC	X	-	Insufficient data		
37	RC	A	A	Insufficient data			Insufficient data					
38	RC	A	A	RC	X	-	RC	X	-	RC	X	-
39	RC	X	-	RC	X	-	A	X	-	RC	X	-
40	RC	X	-	RC	X	-	RC	X	-	RC	X	-

Notation: "LT": Last term of the polynomial equation; "RC": Recalculated; "A": Accepted model; "X": Rejected model; "-": Rejected by the previous criterion.
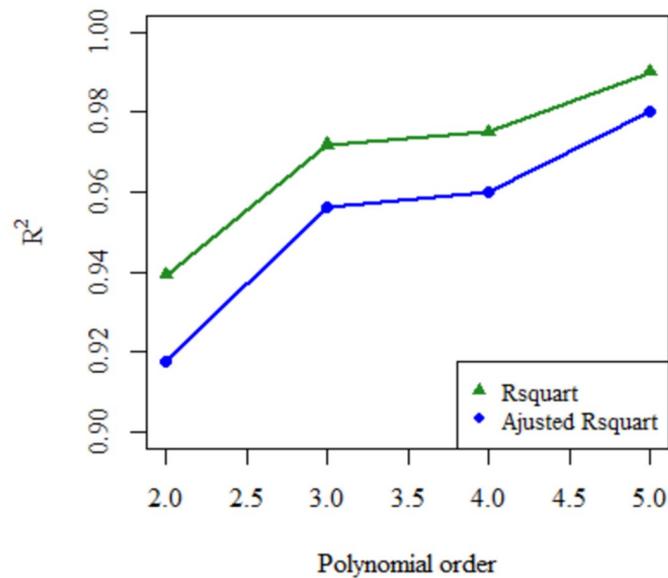
Fig 4. Average of R^2—R^2_a of the data sets fitted to the second to fifth order polynomials.

BIC are likely to minimize information loss, which translates into a more appropriate choice of the model with the best fit [128].

The zero-order model is usually employed to assume a single-phase ideal condition in which the release kinetics is continuous and can be explained as a function dependent on time and independent of the dissolved concentration in the release medium [48]. In addition, zero-order behavior can be observed in materials capable of swelling [129], yet due to complicated bulk erosion and surface erosion and diffusion processes, most studies on the sustained release of hydrophilic drugs have failed to achieve a release profile that conforms to zero-order kinetics for a prolonged time [130]. This conclusion was verified in this study, in which the data sets had a biphasic behavior far from zero-order according to the low values of R^2 and R^2_a and the high averages of the calculated AIC and BIC [131]. Likewise, the results obtained showed rejection of the first-order model for all data sets, demonstrating that the data sets do not follow a model that is dependent on the initial drug concentration [78, 132].

The Korsmeyer-Peppas equation also called "power law" is a semi-empirical model based on the diffusion phenomenon [133] that is used to describe in a general way the main transport phenomena involved in the release, either by diffusion or swelling [134]. Although a good fit has been achieved with this model, several authors have shown that Korsmeyer-Peppas is applicable only to the first 60% of the release profile and is not an appropriate equation to describe the complete release profile [73, 76, 134]. By examining only the first 60% of the data sets, some problems could be detected, such as the small number of observations in some sets, which made it difficult and even impossible to fit the data to the models [135]. It was found that 4 data sets presented a more negative AIC value when 60% of the curve was analyzed, and 6 when 100% was analyzed. This demonstrates that although the model is more complex than the previous ones, this does not result in a better description of the release process.

The empirical Weibull model is an expression that tries to find a linear relationship between the logarithm of drug release and the logarithm of time [136]. Despite not having a kinetic nature, nor parameters physically related to the release phenomena, the ability of the

Table 5. Comparison of R^2 and AIC criteria of data sets using Bootstrap resampling of empirical/semiempirical models and polynomial equations.

| No.	Zero order		First order		Korsmeyer-Peppas 100%		Korsmeyer-Peppas 60%		Weibull		Hyperbolic Tangent		2nd order		3rd order		4th order		5th order	
	R^2	AIC	R^2	AIC	R^2	AIC	R^2	AIC	R^2	AIC	R^2	AIC	R^2	AIC	R^2	AIC	R^2	AIC	R^2	AIC
1	0.68	52.37	0.36	-13.25	0.87	-22.41	0.97	-15.19	0.91	-19.73	0.87	-30.68	0.68	51.5	0.88	49.26	0.68	52.37	0.99	43.16
2	0.68	49.29	0.4	-16.81	0.87	-26.1	0.93	-17.39	0.91	-23.15	0.85	-33.52	0.68	48.32	0.89	45.61	0.68	49.29	1	34.25
3	0.8	57.58	0.54	-23.17	0.98	-55.41	0.97	-52.27	0.99	-58.6	0.96	-67.24	0.8	47.17	0.95	41.68	0.97	34.76	0.97	34.76
4	0.94	23.08	0.85	-11.21	0.98	-15.09	0.95	-16.98	0.99	-20.95	0.9	-23.3	0.97	16.52	1	15.91	Insufficient data		Insufficient data	
5	0.9	22.02	0.79	-11.23	0.88	-14.28	0.88	-14.28	0.96	-15.43	0.98	-23.3	0.94	16.73	1	18.36				
6	0.85	41.55	0.57	-4.86	0.96	-19.35	0.97	-16.73	0.99	-25.41	0.99	-40.32	0.91	40.17	0.72	35.17				
7	0.81	11.62	1	-14.96	0.81	-18.13	Insufficient data		Insufficient data											
8	0.65	20.41	1	-3.8	0.65	-5.61														
9	0.79	19.35	1	-3.45	0.79	-5.71														
10	0.74	31.81	0.6	-2.4	0.92	-8.9			0.96	-9.23	0.98	-19.73	0.99	25.93	1	-12.11				
11	0.9	28.02	0.72	-3.73	0.97	-13.21	0.99	-12.99	0.98	-14.29	0.92	-23.07	0.99	19.53	1	16.45				
12	0.88	55.86	0.59	-14.24	0.94	-28.71	0.83	-13.82	0.96	-22.1	0.96	-34.88	0.88	55.86	0.88	55.86	0.95	53.42	0.99	55.05
13	0.84	51.58	0.61	-20.64	0.98	-46.53	0.98	-46.53	0.98	-44.79	0.95	-58.51	0.84	36.89	0.98	23.08	0.84	51.58	0.99	24.32
14	0.78	43.26	0.59	-19.31	0.97	-37.38	0.97	-20.61	0.99	37.02	0.96	-34.36	0.78	35.05	0.78	35.05	0.78	43.26	0.78	43.26
15	0.73	43.82	0.52	-20.38	0.95	-35.01	1	-15.4	0.98	-33.11	0.94	-30.69	0.73	43.82	0.73	43.82	0.73	43.82	1	17.25
16	0.81	38.89	0.63	-24.77	0.97	-43.47	1	-21.1	0.99	-41.73	0.97	-40.7	0.81	38.89	0.81	38.89	1	28.45	1	19.47
17	0.74	39.87	0.55	-26.04	0.96	-41.2	1	-26.82	0.98	-38.34	0.94	-33.19	0.74	35.13	0.96	32.44	1	22.35	1	9.29
18	0.62	43.12	0.34	2.89	0.6	2.19	Insufficient data		0.47	3.38	0.82	-3.66	0.54	40.22	0.78	42.18	1	40.35	Insufficient data	
19	0.68	49.6	0.32	4.16	0.63	2.7	1	-2.91	0.57	3.32	0.86	-4.56	0.55	46.33	0.97	28.38	1	22.12	1	12.73
20	0.88	48.86	0.65	-28.16	0.98	-64.15	0.98	-64.15	0.98	-62.8	0.99	-100.1	0.88	10.63	0.99	-1.9	0.79	48.86	0.99	1.79
21	0.94	30.67	0.78	-4.34	0.98	-69.71	0.98	-69.71	0.98	-64.97	0.99	-121.2	0.94	-30.87	0.99	-34.67	0.94	30.67	0.94	30.67
22	0.92	40.25	0.73	-38.65	0.98	-66.99	0.98	-66.99	0.98	-61.11	0.99	-104.6	0.92	7.98	0.92	40.25	0.99	8.37	0.99	-2.97
23	0.93	45.66	0.77	-43.02	0.98	-74.29	0.98	-74.29	0.98	-64.26	0.98	-103.8	0.93	-2.83	0.93	45.66	0.99	-3.81	0.93	45.66
24	0.9	42.3	0.71	-38.52	0.99	-81.26	0.99	-81.26	0.99	-79.78	0.98	-109.2	0.9	12.9	0.9	12.9	0.9	12.9	0.9	12.9
25	0.95	43.41	0.79	-41.53	0.98	-74.89	0.98	-74.89	0.98	-63.79	0.98	-107.4	0.95	3.08	0.95	43.41	0.95	43.41	0.95	43.41
26	0.92	27.36	0.79	-46.52	0.95	-54.72	Insufficient data		0.92	-32.7	0.98	-38.03	0.92	27.36	0.92	27.36	0.92	27.36	1	8.18
27	0.85	27.68	0.7	-21.56	0.96	-31.3			0.98	-27.57	0.98	-26.98	0.85	26.4	0.88	21.39	1	5.42	Insufficient data	
28	0.85	32.68	0.66	-11.72	0.96	-21.91	1	-16.76	0.97	-20.11	0.97	-23.01	0.85	27.86	0.99	10.53	1	22.83		
29	0.86	29.37	0.67	-13.71	0.95	-22.55	0.98	-15.33	0.97	-22.12	0.95	-29.74	0.86	27.44	0.95	32.93	1	21.04		
30	0.9	24.04	0.72	-16.39	0.98	-29.01	0.98	-29.01	0.98	-28.44	0.96	-35.77	0.9	21.42	0.9	24.04	1	-5.4		
31	0.86	33.03	0.69	-26.95	0.97	-40.84	0.94	-23.68	0.98	-38.61	0.95	-44.25	0.86	33.03	0.86	33.03	1	26.09	1	24.84
32	0.84	34.88	0.66	-24.77	0.96	-37.54	0.93	-16.67	0.97	-35.32	0.94	-41.95	0.84	34.88	0.84	34.88	1	27.35	1	26.26
33	0.93	22.81	0.8	-9.06	0.97	-19.02	0.97	-19.02	0.98	-20.4	0.99	-41.9	0.93	22.81	0.99	17.67	1	8.1	Insufficient data	
34	0.66	55.04	0.41	-15.52	0.87	-24.93	0.99	-22.07	0.92	-20.17	0.93	-22.17	0.92	-20.17	0.97	46.08	0.98	28.11	0.99	-30.1
35	0.97	31.63	0.87	-25.13	0.99	-56.11	0.99	-27.24	0.96	-21.88	0.63	-13.82	0.97	14.9	0.97	31.63	1	6.42	1	15.4
36	0.9	33.26	0.75	-13.22	0.96	-22.25	Insufficient data		0.67	-6.83	0.94	-10	0.91	33.16	0.98	26.31	0.98	28.11	Insufficient data	
37	0.99	4.43	0.99	-19.04	0.98	-19.04	0.98	-19.04	0.98	-17.37	0.94	-33.26	0.92	13.43	Insufficient data					
38	0.88	30.05	0.65	-11.62	0.96	-23.28	0.96	-23.28	0.87	3.96	0.94	-43.54	0.94	17.63	0.95	16.92	0.99	18.77	1	14.79
39	0.87	30.89	0.66	-11.81	0.97	-25.36	0.97	-25.36	0.84	4.52	0.94	-44.54	0.8	30.89	0.8	30.89	1	4.6	1	7.4
40	0.77	33.1	0.49	3.2	0.9	-4.81	0.9	-4.81	0.91	-4.8	0.94	-42.81	0.77	33.1	0.77	33.1	0.99	17.96	1	15.92
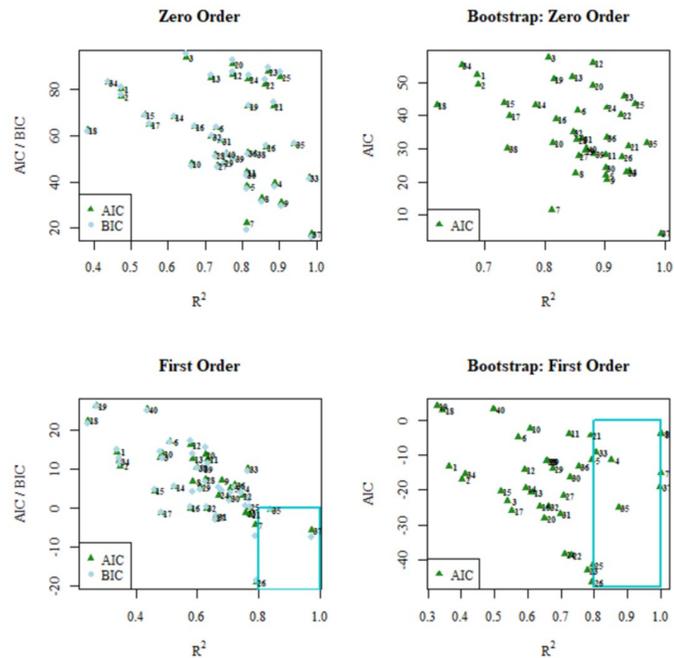
Fig 5. AIC / BIC vs. R^2 plots obtained from linear regression fitting (left) and AIC versus R2 obtained from Bootstrap fitting (right) for the zero-order (top) and first-order (bottom) mathematical models.
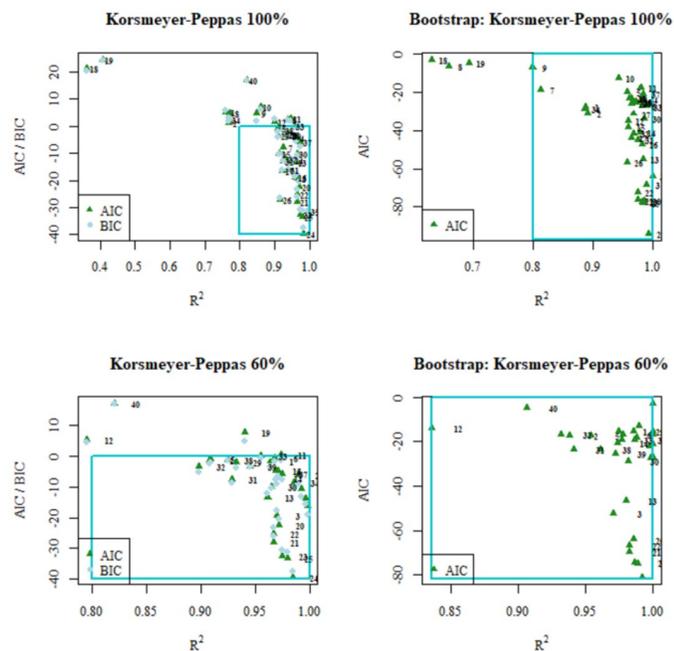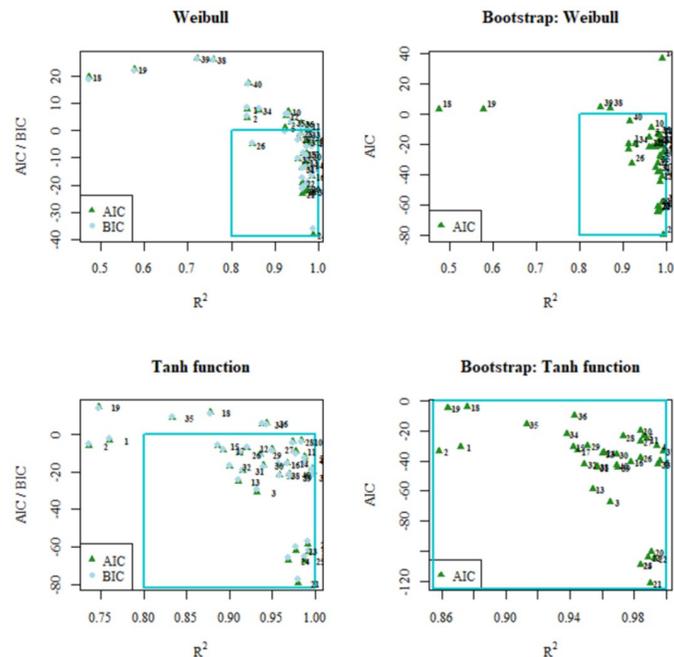
Fig 6. AIC / BIC vs R^2 plots obtained from linear regression fitting (left) and AIC vs R2 obtained from Bootstrap fitting (right) for the mathematical models of Korsmeyer-Peppas fitted to the entire release curve (top) and Korsmeyer-Peppas fitted to the first 60% of the release curve (bottom).

Fig 7. AIC / BIC vs R^2 plots obtained from linear regression fitting (left) and AIC vs R2 obtained from Bootstrap fitting (right) for the mathematical models of Weibull (top) and Hyperbolic Tangent Function (bottom).

https://doi.org/10.1371/journal.pone.0264825.g007

logarithmic form to dampen the abrupt changes in drug concentration rate over time as they pass from one phase to another, has allowed this model to be successfully applied in several release studies [58, 131, 135, 137, 138]. In this study, the Weibull equation was able to fit 12 data sets adequately according to the R^2 and R^2 adjusted, however, when studying the value of AIC and BIC, the model failed to have the best fit in any of the sets, probably because as an empirical model, its predictive power is poor [58, 62, 137]. Weibull has two geometric parameters. The first one is the scale factor "α" which is part of the intercept with the vertical axis, expressed as "ln(α)". The second one is the slope of this equation, usually called "β", is a shape factor of the release curve. Thus, if β = 1, the curve maintains an exponential shape, if β<1 it is considered parabolic and in the case of having a β>1, the shape of the curve is sigmoidal [139]. When analyzing this parameter in the collected data sets (S6 File), a tendency towards a parabolic shape could be observed by obtaining an average of β = 0.71. Sets 8, 9, 18,19, 33, 38 and 39 were the only ones with a sigmoidal curve (β>1) [78]. In order to relate the Weibull model to the predominant transport mechanism in drug release, relationships between the Weibull parameter "β" and the Korsmeyer-Peppas parameter "*n*" have been proposed [140]. Following this theory, Fickian diffusion would be demonstrated when β≤0.75, anomalous transport (diffusion and swelling) when β is between 0.75 and 1, case II type transport when β = 1 and case II type transport which is the combination of phenomena such as diffusion, erosion and macromolecular ratio of polymer chains for the case of cylindrical tablets with β>1 [141, 142]. Doing this analysis with "n" and "β" obtained in this study (S6 File) we obtain a value of "β" to check Fickian diffusion of 0.75, while the transport type case II is explained by β = 1.45. The differences in the ranges could be explained by the difference in the geometry of the DDS [143]. This analysis together with the Korsmeyer-Peppas "n" parameter tests the influence of Fickian diffusion on drug release from PLGA nanoparticles [135].

The hyperbolic tangent function model was the one with the best fit to the experimental data analyzed. This mathematical expression was proposed by Eltayeb et al. in 2016 and is derived from the Korsmeyer-Peppas model, considering diffusion as the main transport phenomenon involved in drug release from nanoparticles [78]. This equation uses the hyperbolic tangent of time as a way to mitigate the abrupt effect of the released drug concentration when its phase changes, similar to the effect of the logarithm in the Weibull model. Unlike Korsmeyer-Peppas, this model can be fitted to the complete release profile and not just to its first 60%. Besides, it is applicable to homogeneous matrices, where the ratio of drug and polymer is equal [73, 76]. From the data sets analyzed, 18 sets were fitted to the hyperbolic tangent model by R^2 and R^2_a and 27 sets considering the AIC and BIC, indicating the model's ability to describe and predict the drug release profile from PLGA nanoparticles synthesized by nanoprecipitation. Being a relatively new model, the physicochemical significance of its parameters is still not fully understood, however, its authors consider that they are related to particle size and diffusion constant [76]. Furthermore, to our knowledge, this model has not been used by other research groups, however, through the analysis performed in this project it is demonstrated that it can be a useful and statistically proven tool to describe release profiles.

As for the four polynomial equations, the importance of the statistical tests to reject the models was evident. Although they showed a good fit measured by R^2 and R^2_a, the increase of these does not indicate a good fit of the model since they tend to increase with the number of variables analyzed in the equation, as shown in Fig 2 [143]. Also, when working with polynomial models, we always try to minimize the number of parameters used in the model since, if the number of parameters is equal to n-1, where n is the number of points to be analyzed, we would obtain an error of fit equal to zero, which is described as an overfitting [144]. Equally, the values of AIC and BIC were more positive compared to the mathematical models. Since AIC and BIC are a measure of goodness-of-fit conditional on the number of parameters used in the model, this result is congruent, and indicates the inability of the expressions to predict the future behavior of the system [131, 145]. Pourtalebi Jahromi and collaborators (2020) used the second degree polynomial equation in their analysis of the release kinetics from nanoparticles, obtaining results similar to those of this study [58]. Nevertheless, no literature was found in which the third-, fourth- or fifth-degree equations were used as a mathematical model in drug release.

On the other hand, the number of observations per set limited in some cases the application of the mathematical models and their statistical tests, especially in sets 7, 8 and 9. In these sets the authors reported the release of 100% of the encapsulated drug in 3 observations. According to Jenkins and Quintana-Ascencia (2020), having a minimum of 8 observations would allow significant statistical conclusions to be reached; however, to increase reproducibility, it is recommended that a minimum of 25 observations be used [146]. From the data sets collected, 50% of them have 8 or more observations, with sets number 20–25 having the most number of observations (14 each set).

When Bootstrap resampling was performed, it was possible to determine the model that best fit the data sets 7, 8 and 9. It proves that this technique can be a powerful tool when there is a limited number of observations. The results with this method were similar to the raw data, obtaining that 70% of the data sets fit the Hyperbolic Tangent model.

Conclusions

This study demonstrated that, although they are tools that help to understand drug release dynamics, there is no general empirical/semiempirical mathematical expression that can describe, in all cases, the release profile of drugs encapsulated in PLGA nanoparticles

synthesized by nanoprecipitation methods. In addition, it was found that although R^2 and R^2_a are the most commonly used criteria to determine whether or not a model fits the data obtained in an experiment, they are not the most appropriate. It was also shown that the Akaike and Bayesian criteria can better reflect the fit of a model since the results are not influenced by the inclusion of new terms or an increase in the complexity of the equation. It was also revealed that the number of observations per set is a limiting factor for the application of different models and the subsequent statistical analysis. Therefore, the Bootstrap resampling technique becomes a very useful technique to solve this drawback. In the specific case of this study, 50% of the sets studied do not meet the requirement of at least 8 observations for the construction of the release curve, therefore these results are not very reproducible and have low statistical significance.

Furthermore, the analysis employed in this project provided significant statistical evidence to consider the Hyperbolic Tangent Function model as the most adequate and general model to describe the drug release kinetics. This model, unlike the mathematical expression of Korsmeyer-Peppas, could be adjusted to the complete release curve. Since it has kinetic parameters, it acquires greater predictive power than the Weibull model. However, a more exhaustive study of this model is required in order to understand the chemistry, physics, and biology behind it.

Supporting information

S1 File. Equations of second to fifth order polynomials and Equations for the mathematical model acceptance criteria.
(DOCX)

S2 File. Release kinetic data. Forty sets of cumulative drug release data obtained from different scientific articles published in scientific journals since 2016 are listed below. It is included, if available, the model that best fits each set according to the authors.
(DOCX)

S3 File. R programming. This appendix shows the programming models in the statistical program R. For this purpose, set number 33 [109] and its fit to the Korsmeyer-Peppas model was taken as an example.
(DOCX)

S4 File. Results of the fit and the acceptance criteria for each studied mathematical model and polynomial.
(DOCX)

S5 File. Bootstrapping fitted regression for each studied mathematical model and polynomial.
(DOCX)

S6 File. Linear regression of β vs. n. In order to give significance to the Weibull method, a linear regression was performed between the Korsmeyer-Peppas n parameter and the Weibull beta parameter.
(DOCX)

Acknowledgments

Author Contributions

Conceptualization: Karla Vizuete, Alexis Debut.

Data curation: Nathaly S. Heredia, Karla Vizuete.

Formal analysis: Nathaly S. Heredia, Karla Vizuete.

Methodology: Nathaly S. Heredia, Karla Vizuete, Marco Flores-Calero, Katherine Pazmiño V., Alexis Debut.

Software: Nathaly S. Heredia.

Supervision: Karla Vizuete, Marco Flores-Calero, Fernanda Pilaquinga, Brajesh Kumar.

Validation: Karla Vizuete, Katherine Pazmiño V., Fernanda Pilaquinga, Brajesh Kumar, Alexis Debut.

Writing – original draft: Nathaly S. Heredia, Karla Vizuete, Alexis Debut.

Writing – review & editing: Karla Vizuete, Marco Flores-Calero, Katherine Pazmiño V., Fernanda Pilaquinga, Brajesh Kumar, Alexis Debut.

References

1. Farokhzad OC, Langer R. Impact of Nanotechnology on Drug Delivery. ACS Nano. 2009; 3: 16–20. https://doi.org/10.1021/nn900002m PMID: 19206243

2. Parveen S, Sahoo SK. Polymeric nanoparticles for cancer therapy. J Drug Target. 2008; 16: 108–123. https://doi.org/10.1080/10611860701794353 PMID: 18274932

3. Wagner V, Dullaart A, Bock AK, Zweck A. The emerging nanomedicine landscape. Nat Biotechnol. 2006; 24: 1211–1217. https://doi.org/10.1038/nbt1006-1211 PMID: 17033654

4. Cukierman E, Khan DR. The benefits and challenges associated with the use of drug delivery systems in cancer therapy. Biochem Pharmacol. 2010; 80: 762–770. https://doi.org/10.1016/j.bcp.2010.04.020 PMID: 20417189

5. Ghitman J, Biru EI, Stan R, Iovu H. Review of hybrid PLGA nanoparticles: Future of smart drug delivery and theranostics medicine. Mater Des. 2020; 193: 108805. https://doi.org/10.1016/j.matdes.2020.108805

6. Jo MJ, Jin IS, Park CW, Hwang BY, Chung YB, Kim JS, et al. Revolutionizing technologies of nanomicelles for combinatorial anticancer drug delivery. Arch Pharm Res. 2020; 43: 100–109. https://doi.org/10.1007/s12272-020-01215-4 PMID: 31989478

7. Joseph RR, Venkatraman SS. Drug delivery to the eye: What benefits do nanocarriers offer? Nanomedicine. 2017; 12: 683–702. https://doi.org/10.2217/nnm-2016-0379 PMID: 28186436

8. Lopez FL, Ernest TB, Tuleu C, Gul MO. Formulation approaches to pediatric oral drug delivery: Benefits and limitations of current platforms. Expert Opin Drug Deliv. 2015; 12: 1727–1740. https://doi.org/10.1517/17425247.2015.1060218 PMID: 26165848

9. Netti PA, Biondi M, Frigione M. Experimental studies and modeling of the degradation process of poly (lactic-co-glycolic acid) microspheres for sustained protein release. Polymers (Basel). 2020; 12. https://doi.org/10.3390/polym12092042 PMID: 32911693

10. Safari J, Zarnegar Z. Advanced drug delivery systems: Nanotechnology of health design A review. J Saudi Chem Soc. 2014; 18: 85–99. https://doi.org/10.1016/j.jscs.2012.12.009

11. Snejdrova E, Podzimek S, Martiska J, Holas O, Dittrich M. Branched PLGA derivatives with tailored drug delivery properties. Acta Pharm. 2020; 70: 63–75. https://doi.org/10.2478/acph-2020-0011 PMID: 31677370

12. Moritera T, Ogura Y, Honda Y, Wada R, Hyon SH, Ikada Y. Microspheres of biodegradable polymers as a drug-delivery system in the vitreous. Invest Ophthalmol Vis Sci. 1991; 32: 1785–1790. Available from: https://iovs.arvojournals.org/article.aspx?articleid=2178814 PMID: 2032801

13. Kaity S, Maiti S, Ghosh AK, Pal D, Ghosh A, Banerjee S. Microsponges: A novel strategy for drug delivery system. J Adv Pharm Technol Res. 2010; 1: 283. https://doi.org/10.4103/0110-5558.72416 PMID: 22247859

14. Bariya SH, Gohel MC, Mehta TA, Sharma OP. Microneedles: an emerging transdermal drug delivery system. J Pharm Pharmacol. 2011; 64: 11–29. https://doi.org/10.1111/j.2042-7158.2011.01369.x PMID: 22150668

15. Weiner N, Martin F, Riaz M. Liposomes as a Drug Delivery System. Drug Dev Ind Pharm. 1989; 15: 1523–1554. https://doi.org/10.3109/03639048909052502

16. Rajera R, Nagpal K, Singh SK, Mishra DN. Niosomes: A controlled and novel drug delivery system. Biol Pharm Bull. 2011; 34: 945–953. https://doi.org/10.1248/bpb.34.945 PMID: 21719996

17. Amina SJ, Guo B. A Review on the Synthesis and Functionalization of Gold Nanoparticles as a Drug Delivery Vehicle. Int J Nanomedicine. 2020; 15: 9823. https://doi.org/10.2147/IJN.S279094 PMID: 33324054

18. Mou X, Ali Z, Li S, He N. Applications of magnetic nanoparticles in targeted drug delivery system. J Nanosci Nanotechnol. 2015; 15: 54–62. https://doi.org/10.1166/jnn.2015.9585 PMID: 26328305

19. Gao L, Zhang D, Chen M. Drug nanocrystals for the formulation of poorly soluble drugs and its application as a potential drug delivery system. J Nanoparticle Res. 2008; 10: 845–862. https://doi.org/10.1007/s11051-008-9357-4

20. Huang H, Yuan Q, Shah JS, Misra RDK. A new family of folate-decorated and carbon nanotube-mediated drug delivery system: Synthesis and drug delivery response. Adv Drug Deliv Rev. 2011; 63: 1332–1339. https://doi.org/10.1016/j.addr.2011.04.001 PMID: 21514336

21. Kibria G, Ramos EK, Wan Y, Gius DR, Liu H. Exosomes as a Drug Delivery System in Cancer Therapy: Potential and Challenges. Mol Pharm. 2018; 15: 3625–3633. https://doi.org/10.1021/acs.molpharmaceut.8b00277 PMID: 29771531

22. Liu D, Yang F, Xiong F, Gu N. The smart drug delivery system and its clinical potential. Theranostics. Ivyspring International Publisher; 2016. pp. 1306–1323. https://doi.org/10.7150/thno.14858 PMID: 27375781

23. Elmowafy EM, Tiboni M, Soliman ME. Biocompatibility, biodegradation and biomedical applications of poly(lactic acid)/poly(lactic-co-glycolic acid) micro and nanoparticles. J Pharm Investig. 2019; 49: 347–380. https://doi.org/10.1007/s40005-019-00439-x

24. Naahidi S, Jafari M, Edalat F, Raymond K, Khademhosseini A, Chen P. Biocompatibility of engineered nanoparticles for drug delivery. J Control Release. 2013; 166: 182–194. https://doi.org/10.1016/j.jconrel.2012.12.013 PMID: 23262199

25. Joshi JR, Patel RP. Role of biodegradable polymers in drug delivery. Int J Curr Pharm Res. 2012; 4: 74–81. Available from: https://innovareacademics.in/journal/ijcpr/Issues/Vol4Issue4/603.pdf

26. Pillai O, Panchagnula R. Polymers in drug delivery. Curr Opin Chem Biol. 2001; 5: 447–451. https://doi.org/10.1016/s1367-5931(00)00227-1 PMID: 11470609

27. Locatelli E, Comes Franchini M. Biodegradable PLGA-b-PEG polymeric nanoparticles: synthesis, properties, and nanomedical applications as drug delivery system. J Nanoparticle Res. 2012; 14: 1316. https://doi.org/10.1007/s11051-012-1316-4

28. Makadia HK, Siegel SJ. Poly Lactic-co-Glycolic Acid (PLGA) as Biodegradable Controlled Drug Delivery Carrier. Polymers (Basel). 2011; 3: 1377–1397. https://doi.org/10.3390/polym3031377 PMID: 22577513

29. Danhier F, Ansorena E, Silva JM, Coco R, Le Breton A, Préat V. PLGA-based nanoparticles: An overview of biomedical applications. J Control Release. 2012; 161: 505–522. https://doi.org/10.1016/j.jconrel.2012.01.043 PMID: 22353619

30. Fredenberg S, Wahlgren M, Reslow M, Axelsson A. The mechanisms of drug release in poly(lactic-co-glycolic acid)-based drug delivery systems—A review. Int J Pharm. 2011; 415: 34–52. https://doi.org/10.1016/j.ijpharm.2011.05.049 PMID: 21640806

31. Chasin M, Langer R. Biodegradable polymers as drug delivery systems. Drug Development and Industrial Pharmacy. New York, NY: Marcel Dekker Inc.; 1991.

32. Xu Y, Kim CS, Saylor DM, Koo D. Polymer degradation and drug delivery in PLGA-based drug–polymer applications: A review of experiments and theories. J Biomed Mater Res—Part B Appl Biomater. 2017; 105: 1692–1716. https://doi.org/10.1002/jbm.b.33648 PMID: 27098357

33. Liang X, Duan P, Gao J, Guo R, Qu Z, Li X, et al. Bilayered PLGA/PLGA-HAp Composite Scaffold for Osteochondral Tissue Engineering and Tissue Regeneration. ACS Biomater Sci Eng. 2018; 4: 3506–3521. https://doi.org/10.1021/acsbiomaterials.8b00552 PMID: 33465902

34. Lee S-J, Kim H-J, Huh Y-M, Kim IW, Jeong JH, Kim J-C, et al. Functionalized Magnetic PLGA Nanospheres for Targeting and Bioimaging of Breast Cancer. J Nanosci Nanotechnol. 2017; 18: 1542–1547. https://doi.org/10.1166/jnn.2018.14220 PMID: 29448628

35. Pazmiño V. K, Vizuete KS, Alexis F, Kumar B, Debut A. A Closer Look to Polyesters: Properties, Synthesis, Characterization, and Particle Drug Delivery Applications. Nanosci Nanotechnology-Asia. 2020; 10. https://doi.org/10.2174/2210681210999201124155313

36. Lü JM, Wang X, Marin-Muller C, Wang H, Lin PH, Yao Q, et al. Current advances in research and clinical applications of PLGA-based nanotechnology. Expert Review of Molecular Diagnostics. 2009. pp. 325–341. https://doi.org/10.1586/erm.09.15 PMID: 19435455

37. Chopra S, Bertrand N, Lim JM, Wang A, Farokhzad OC, Karnik R. Design of Insulin-Loaded Nanoparticles Enabled by Multistep Control of Nanoprecipitation and Zinc Chelation. ACS Appl Mater Interfaces. 2017; 9: 11440–11450. https://doi.org/10.1021/acsami.6b16854 PMID: 28323414

38. Pandey A, Jain DS. Poly Lactic-Co-Glycolic Acid (PLGA) Copolymer and Its Pharmaceutical Application. Handb Polym Pharm Technol. 2015; 2: 151–172. https://doi.org/10.1002/9781119041412.ch6

39. Sharma S, Parmar A, Kori S, Sandhir R. PLGA-based nanoparticles: A new paradigm in biomedical applications. TrAC—Trends Anal Chem. 2016; 80: 30–40. https://doi.org/10.1016/j.trac.2015.06.014

40. Ye M, Duan H, Yao L, Fang Y, Zhang X, Dong L, et al. A method of elevated temperatures coupled with magnetic stirring to predict real time release from long acting progesterone PLGA microspheres. Asian J Pharm Sci. 2019; 14: 222–232. https://doi.org/10.1016/j.ajps.2018.05.010 PMID: 32104454

41. Zhang L, Wang Z, Xiao Y, Liu P, Wang S, Zhao Y, et al. Electrospun PEGylated PLGA nanofibers for drug encapsulation and release. Mater Sci Eng C. 2018; 91: 255–262. https://doi.org/10.1016/j.msec.2018.05.045 PMID: 30033253

42. Serris I, Serris P, Frey KM, Cho H. Development of 3D-Printed Layered PLGA Films for Drug Delivery and Evaluation of Drug Release Behaviors. AAPS PharmSciTech. 2020; 21. https://doi.org/10.1208/s12249-020-01790-1 PMID: 32888114

43. Milovanovic S, Markovic D, Mrakovic A, Kuska R, Zizovic I, Frerich S, et al. Supercritical CO 2—assisted production of PLA and PLGA foams for controlled thymol release. Mater Sci Eng C. 2019; 99: 394–404. https://doi.org/10.1016/j.msec.2019.01.106 PMID: 30889714

44. Ahmed T, Aljaeid B. A potential in situ gel formulation loaded with novel fabricated poly(lactide-co-glycolide) nanoparticles for enhancing and sustaining the ophthalmic delivery of ketoconazole. Int J Nanomedicine. 2017; Volume 12: 1863–1875. https://doi.org/10.2147/IJN.S131850 PMID: 28331311

45. Anwer MK, Jamil S, Ansari MJ, Iqbal M, Imam F, Shakeel F. Development and evaluation of olmesartan medoxomil loaded PLGA nanoparticles. Mater Res Innov. 2016; 20: 193–197. https://doi.org/10.1179/1433075X15Y.0000000049

46. Vakilinezhad MA, Amini A, Dara T, Alipour S. Methotrexate and Curcumin co-encapsulated PLGA nanoparticles as a potential breast cancer therapeutic system: In vitro and in vivo evaluation. Colloids Surfaces B Biointerfaces. 2019; 184: 110515. https://doi.org/10.1016/j.colsurfb.2019.110515 PMID: 31585308

47. Patra JK, Das G, Fraceto LF, Campos EVR, Rodriguez-Torres MDP, Acosta-Torres LS, et al. Nano based drug delivery systems: Recent developments and future prospects. Journal of Nanobiotechnology. BioMed Central Ltd.; 2018. p. 71. https://doi.org/10.1186/s12951-018-0392-8 PMID: 30231877

48. Yoo J, Won YY. Phenomenology of the Initial Burst Release of Drugs from PLGA Microparticles. ACS Biomater Sci Eng. 2020; 6: 6053–6062. https://doi.org/10.1021/acsbiomaterials.0c01228 PMID: 33449671

49. Yu JH, Brown J, Boisseau N, Barthel T, Murray S. Effects of Lupron and surgical castration on fecal androgen metabolite concentrations and intermale aggression in capybaras (Hydrochoerus hydrochaeris). Zoo Biol. 2021; 40: 135–141. https://doi.org/10.1002/zoo.21586 PMID: 33338298

50. Ogawa Y, Yamamoto M, Okada H, Yashiki T, Shimamoto T. A new technique to efficiently entrap leuprolide acetate into microcapsules of polylactic acid or copoly(lactic/glycolic) acid. Chem Pharm Bull (Tokyo). 1988; 36: 1095–1103. https://doi.org/10.1248/cpb.36.1095 PMID: 3136939

51. Okada H, Doken Y, Ogawa Y, Toguchi H. Preparation of three-month depot injectable microspheres of leuprorelin acetate using biodegradable polymers. Pharm Res. 1994; 11: 1143–7. https://doi.org/10.1023/a:1018936815654 PMID: 7971715

52. Klein K, Yang J, Aisenberg J, Wright N, Kaplowitz P, Lahlou N, et al. Efficacy and safety of triptorelin 6-month formulation in patients with central precocious puberty. J Pediatr Endocrinol Metab. 2016; 29: 1241–1248. https://doi.org/10.1515/jpem-2015-0376 PMID: 26887034

53. Kumskova N, Ermolenko Y, Osipova N, Semyonkin A, Kildeeva N, Gorshkova M, et al. How subtle differences in polymer molecular weight affect doxorubicin-loaded PLGA nanoparticles degradation and drug release. J Microencapsul. 2020; 37: 283–295. https://doi.org/10.1080/02652048.2020.1729885 PMID: 32079451

54. Lagreca E, Onesto V, Di Natale C, La Manna S, Netti PA, Vecchione R. Recent advances in the formulation of PLGA microparticles for controlled drug delivery. Prog Biomater. 2020; 9: 153–174. https://doi.org/10.1007/s40204-020-00139-y PMID: 33058072

55. Atif R, Salah Eldeen T, Yahya I, Ahmed L, Omara A, Eltayeb M. Mathematical Modeling of Diffusion Controlled Drug Release Profiles from Nanoparticles. Int J Res Sci Innov |. 2019; VI: 287–291. Available from: www.rsisinternational.org

56. Alexis F. Factors affecting the degradation and drug-release mechanism of poly(lactic acid) and poly [(lactic acid)-co-(glycolic acid)]. Polym Int. 2005; 54: 36–46. https://doi.org/10.1002/pi.1697

57. Alexis F, Santosh Kumar R, Venkatraman SS, Frank A, Rath SK, Venkatraman SS. Controlled release from bioerodible polymers: effect of drug type and polymer composition. J Control Release. 2005; 102: 333–344. https://doi.org/10.1016/j.jconrel.2004.10.019 PMID: 15653155

58. Pourtalebi Jahromi L, Ghazali M, Ashrafi H, Azadi A. A comparison of models for the analysis of the kinetics of drug release from PLGA-based nanoparticles. Heliyon. 2020; 6. https://doi.org/10.1016/j.heliyon.2020.e03451 PMID: 32140583

59. Tamani F, Hamoudi MC, Danede F, Willart JF, Siepmann F, Siepmann J. Towards a better understanding of the release mechanisms of caffeine from PLGA microparticles. J Appl Polym Sci. 2020; 137: 1–12. https://doi.org/10.1002/app.48710

60. Alexis F, Venkatraman S, Kumar Rath S, Gan L-HH, Rath SK, Gan L-HH. Some insight into hydrolytic scission mechanisms in bioerodible polyesters. J Appl Polym Sci. 2006; 102: 3111–3117. https://doi.org/10.1002/app.23888

61. Huang X, Brazel CS. On the importance and mechanisms of burst release in matrix-controlled drug delivery systems. J Control Release. 2001; 73: 121–136. https://doi.org/10.1016/s0168-3659(01)00248-6 PMID: 11516493

62. Hines DJ, Kaplan DL. Poly (lactic-co-glycolic acid) controlled release systems: experimental and modeling insights. Crit Rev Ther Drug Carrier Syst. 2013; 30: 257–276. https://doi.org/10.1615/critrevtherdrugcarriersyst.2013006475 PMID: 23614648

63. Ford Versypt AN, Pack DW, Braatz RD. Mathematical modeling of drug delivery from autocatalytically degradable PLGA microspheres—A review. J Control Release. 2013; 165: 29–37. https://doi.org/10.1016/j.jconrel.2012.10.015 PMID: 23103455

64. Casalini T, Rossi F, Lazzari S, Perale G, Masi M. Mathematical modeling of PLGA microparticles: From polymer degradation to drug release. Mol Pharm. 2014; 11: 4036–4048. https://doi.org/10.1021/mp500078u PMID: 25230105

65. Schoubben A, Ricci M, Giovagnoli S. Meeting the unmet: from traditional to cutting-edge techniques for poly lactide and poly lactide-co-glycolide microparticle manufacturing. J Pharm Investig. 2019; 49: 381–404. https://doi.org/10.1007/s40005-019-00446-y

66. Hua Y, Wang Z, Wang D, Lin X, Liu B, Zhang H, et al. Key Factor Study for Generic Long-Acting PLGA Microspheres Based on a Reverse Engineering of Vivitrol®. Molecules. 2021; 26. https://doi.org/10.3390/molecules26051247 PMID: 33669152

67. Grassi M, Grassi G. Application of mathematical modeling in sustained release delivery systems. Expert Opin Drug Deliv. 2014; 11: 1299–1321. https://doi.org/10.1517/17425247.2014.924497 PMID: 24938598

68. Siepman J, Göpferich A. Mathematical modeling of bioerodible, polymeric drug delivery systems. Adv Drug Deliv Rev. 2001; 48: 229–247. https://doi.org/10.1016/s0169-409x(01)00116-8 PMID: 11369084

69. Lopina ST, Kanjickal DG. Modeling of Drug Release from Polymeric Delivery Systems?A Review; Crit Rev Ther Drug Carrier Syst. 2004; 21: 345–386. https://doi.org/10.1615/critrevtherdrugcarriersyst.v21.i5.10 PMID: 15717734

70. Mircioiu C, Voicu V, Anuta V, Tudose A, Celia C, Paolino D, et al. Mathematical Modeling of Release Kinetics from Supramolecular Drug Delivery Systems. Pharmaceutics. 2019; 11: 140. https://doi.org/10.3390/pharmaceutics11030140 PMID: 30901930

71. Yamuna M, Elakkiya A. Mathematical Models in Drug Discovery, Development and Treatment of Various Diseases-A Case Study. Res J Pharm Technol. 2017; 10: 4397. https://doi.org/10.5958/0974-360x.2017.00810.1

72. Alencastre I, Sousa D, Alves C, Leitão L, Neto E, Aguiar P, et al. Delivery of pharmaceutics to bone: nanotechnologies, high-throughput processing and in silico mathematical models. Eur Cells Mater. 2016; 31: 355–381. https://doi.org/10.22203/eCM.v031a23

73. Ahmed L, Atif R, Eldeen TS, Yahya I, Omara A, Eltayeb M. Study the Using of Nanoparticles as Drug Delivery System Based on Mathematical Models for Controlled Release. IJLTEMAS. 2019. Available from: www.ijltemas.in

74. Siepmann J, Siepmann F, Florence AT. Local controlled drug delivery to the brain: Mathematical modeling of the underlying mass transport mechanisms. Int J Pharm. 2006; 314: 101–119. https://doi.org/10.1016/j.ijpharm.2005.07.027 PMID: 16647231

75. Kim G, Kim HJ, Noh H. Influence of Solution pH on Drug Release from Ionic Hydrogel Lens. Macromol Res. 2019; 27: 191–197. https://doi.org/10.1007/s13233-019-7050-3

76. Eltayeb M, Stride E, Edirisinghe M, Harker A. Electrosprayed nanoparticle delivery system for controlled release. Mater Sci Eng C. 2016; 66: 138–146. https://doi.org/10.1016/j.msec.2016.04.001 PMID: 27207047

77. Costa P, Sousa Lobo JM. Modeling and comparison of dissolution profile. Eur J Pharm Sci. 2001; 13: 123–133. https://doi.org/10.1016/s0928-0987(01)00095-1 PMID: 11297896

78. Ramteke K, Dighe P, K A., Patil S. Mathematical models of drug dissolution: A review. Sch Acad Sci Publ. 2014; 388–396. Available from: https://saspublishers.com/media/articles/SAJP35388-396.pdf

79. Korsmeyer RW, Gurny R, Doelker E, Buri P, Peppas NA. Mechanisms of solute release from porous hydrophilic polymers. Int J Pharm. 1983; 15: 25–35. https://doi.org/10.1016/0378-5173(83)90064-9

80. Bruschi M. Mathematical models of drug release. Strategies to Modify the Drug Release from Pharmaceutical Systems. Elsevier Ltd; 2015. pp. 63–86.

81. Peppas NA. Analysis of Fickian and non-Fickian drug release from polymers. Pharm Acta Helv. 1985; 60: 110–111. Available from: https://europepmc.org/article/MED/4011621 PMID: 4011621

82. Higuchi T. Rate of Release of Medicaments from Ointment Bases Containing Drugs in Suspension. J Pharm Sci. 1961; 50: 874–875. https://doi.org/10.1002/jps.2600501018 PMID: 13907269

83. Langenbucher F. Letters to the Editor: Linearization of dissolution rate curves by the Weibull distribution. J Pharm Pharmacol. 1972; 24: 979–981. https://doi.org/10.1111/j.2042-7158.1972.tb08930.x PMID: 4146531

84. Weibull W. A Statistical Distribution Function of Wide Applicability. J Appl Mech. 1951; 18: 293–297.

85. Hopfenberg H. Controlled release from erodible slabs, cylinders, and spheres. In: Paul DR, Harris FW, editors. Controlled Release Polymeric Formulations. Washington: ACS; 1976. pp. 26–32.

86. Ağabeyoğlu I. T., & Ecz. Fak. AÜ. Studies on sustained release IV: inert matrix tablets of sulfamethizole, employing polyvinyl chloride and carboxypolymemylene. Drug Dev Ind Pharm. 2021; 2: 2013–2015.

87. Core R Team. A Language and Environment for Statistical Computing. Version 1.3.1093 [software]. R Foundation for Statistical Computing. Vienna: R Foundation for Statistical Computing; 2018. http://www.r-project.org/

88. Faraway J. Practical Regression and Anova using R. Computers and Education. University of Bath; 2002.

89. Anderson DR, Sweeney DJ, Williams TA. Estadística para administración y economía. 10th ed. Cengace Learning S.A.; 2008.

90. Robinson D. broom: An R package for converting statistical analysis objects into tidy data frames. arXiv:14123565v2. 2014. http://arxiv.org/abs/1412.3565

91. Bland JM, Altman DG. Statistics Notes: Bootstrap resampling methods. Res methods Report. 2015; 2–3. https://doi.org/10.1136/bmj.h2622 PMID: 26037412

92. Dixon PM. Bootstrap resampling. Encycl environmetrics. 2006. https://doi.org/10.1002/9780470057339.vab028

93. Fox J, Weisberg S, Price B. Package "carData" 2020. In: Version 3.0–4. [software] CRAN [Internet]. 2018 [cited 22 Feb 2021]. https://cran.r-project.org/package=carData

94. Fox J, Weisberg S. Using car and effects Functions in Other Functions. 2020; 3: 1–5.

95. Barton K. MuMIn: Multi-Model Inference. R package version 1.43.17. Version. 2020;1: 18. https://cran.r-project.org/package=MuMIn

96. Rizopoulos D. Package "bootStepAIC." R Packag Version 12–0 [software] CRAN. 2009; 1–5. https://cran.r-project.org/web/packages/bootStepAIC/bootStepAIC.pdf

97. Venables WN, Ripley BD. Modern Applied Statistics with S. New York: Springer; 2002.

98. Yuan X, Ji W, Chen S, Bao Y, Tan S, Lu S, et al. Anovel paclitaxel-loaded poly(D,L-lactide-co-glycolide)-Tween 80 copolymer nanoparticle overcoming multidrug resistance for lung cancer treatment. Int J Nanomedicine. 2016; 11: 2119–2131. https://doi.org/10.2147/IJN.S92271 PMID: 27307727

99. Zhang M, He J, Zhang W, Liu J. Fabrication of TPGS-Stabilized Liposome-PLGA Hybrid Nanoparticle Via a New Modified Nanoprecipitation Approach: In Vitro and In Vivo Evaluation. Pharm Res. 2018; 35. https://doi.org/10.1007/s11095-018-2485-3 PMID: 30167890

100. Han FY, Liu Y, Kumar V, Xu W, Yang G, Zhao CX, et al. Sustained-release ketamine-loaded nanoparticles fabricated by sequential nanoprecipitation. Int J Pharm. 2020;581. https://doi.org/10.1016/j.ijpharm.2020.119291 PMID: 32259638

101. Kandilli B, Ugur Kaplan AB, Cetin M, Taspinar N, Ertugrul MS, Aydin IC, et al. Carbamazepine and levetiracetam-loaded PLGA nanoparticles prepared by nanoprecipitation method: in vitro and in vivo studies. Drug Dev Ind Pharm. 2020; 46: 1063–1072. https://doi.org/10.1080/03639045.2020.1769127 PMID: 32406290

102. Sahin A, Spiroux F, Guedon I, Arslan FB, Sarcan ET, Ozkan T, et al. Using PVA and TPGS as combined emulsifier in nanoprecipitation method improves characteristics and anticancer activity of ibuprofen loaded PLGA nanoparticles. Pharmazie. 2017; 72: 525–528. https://doi.org/10.1691/ph.2017.7015 PMID: 29441979

103. Sahin A, Esendagli G, Yerlikaya F, Caban-Toktas S, Yoyen-Ermis D, Horzum U, et al. A small variation in average particle size of PLGA nanoparticles prepared by nanoprecipitation leads to considerable change in nanoparticles' characteristics and efficacy of intracellular delivery. Artif Cells, Nanomedicine Biotechnol. 2017; 45: 1657–1664. https://doi.org/10.1080/21691401.2016.1276924 PMID: 28084837

104. Chiesa E, Dorati R, Modena T, Conti B, Genta I. Multivariate analysis for the optimization of microfluidics-assisted nanoprecipitation method intended for the loading of small hydrophilic drugs into PLGA nanoparticles. Int J Pharm. 2018; 536: 165–177. https://doi.org/10.1016/j.ijpharm.2017.11.044 PMID: 29175645

105. Albisa A, Piacentini E, Sebastian V, Arruebo M, Santamaria J, Giorno L. Preparation of Drug-Loaded PLGA-PEG Nanoparticles by Membrane-Assisted Nanoprecipitation. Pharm Res. 2017; 34: 1296–1308. https://doi.org/10.1007/s11095-017-2146-y PMID: 28342057

106. Donno R, Gennari A, Lallana E, De La Rosa JMR, d'Arcy R, Treacher K, et al. Nanomanufacturing through microfluidic-assisted nanoprecipitation: Advanced analytics and structure-activity relationships. Int J Pharm. 2017; 534: 97–107. https://doi.org/10.1016/j.ijpharm.2017.10.006 PMID: 29017804

107. Liu D, Zhang H, Cito S, Fan J, Mäkilä E, Salonen J, et al. Core/Shell Nanocomposites Produced by Superfast Sequential Microfluidic Nanoprecipitation. Nano Lett. 2017; 17: 606–614. https://doi.org/10.1021/acs.nanolett.6b03251 PMID: 28060521

108. Balla A, Goli D. Formulation & evaluation of PLGA nanoparticles of ropinirole HCl for targeting brain. Indian J Pharm Sci. 2020; 82: 622–631. https://doi.org/10.36468/pharmaceutical-sciences.688

109. Xu J, Chen Y, Jiang X, Gui Z, Zhang L. Development of hydrophilic drug encapsulation and controlled release using a modified nanoprecipitation method. Processes. 2019; 7. https://doi.org/10.3390/pr7060331

110. Jamali Z, Khoobi M, Hejazi SM, Eivazi N, Abdolahpour S, Imanparast F, et al. Evaluation of targeted curcumin (CUR) loaded PLGA nanoparticles for in vitro photodynamic therapy on human glioblastoma cell line. Photodiagnosis Photodyn Ther. 2018; 23: 190–201. https://doi.org/10.1016/j.pdpdt.2018.06.026 PMID: 29969678

111. Darwish WMA, Bayoumi NA. Gold nanorod–loaded (PLGA-PEG) nanocapsules as near-infrared controlled release model of anticancer therapeutics. Lasers Med Sci. 2020; 35: 1729–1740. https://doi.org/10.1007/s10103-020-02964-w PMID: 31965353

112. Alsulays BB, Anwer MK, Aldawsari MF, Aodah A, Adam E, Alshehri S, et al. Preparation and evaluation of a stable and sustained release of lansoprazole-loaded poly(d,l-lactide-co-glycolide) polymeric nanoparticles. J Polym Eng. 2019; 39: 822–829. https://doi.org/10.1515/polyeng-2019-0164

113. Sivaprasad S, Bose C, Sadakvali C, Ravi G, Swathi V. Formulation and characterization of saquinavir nanoparticles prepared by nanoprecipitation method. World J Pharm Res. 2020. https://doi.org/10.20959/wjpr20205-17476

114. Liu Y, Yang G, Baby T, Tengjisi Chen D, Weitz DA, et al. Stable Polymer Nanoparticles with Exceptionally High Drug Loading by Sequential Nanoprecipitation. Angew Chemie—Int Ed. 2020; 59: 4720–4728. https://doi.org/10.1002/anie.201913539

115. Amini-Fazl MS, Mobedi H. Investigation of mathematical models based on diffusion control release for Paclitaxel from in-situ forming PLGA microspheres containing HSA microparticles. Mater Technol. 2020; 35: 50–59. https://doi.org/10.1080/10667857.2019.1651549

116. Bhattacharjee S. Understanding the burst release phenomenon: Toward designing effective nanoparticulate drug-delivery systems. Therapeutic Delivery. Future Medicine Ltd.; 2021. pp. 21–36. https://doi.org/10.4155/tde-2020-0099 PMID: 33353422

117. Sevim K, Pan J. A Mechanistic Model for Acidic Drug Release Using Microspheres Made of PLGA 50:50. Mol Pharm. 2016; 13: 2729–2735. https://doi.org/10.1021/acs.molpharmaceut.6b00313 PMID: 27398973

118. Busatto C, Pesoa J, Helbling I, Luna J, Estenoz D. Effect of particle size, polydispersity and polymer degradation on progesterone release from PLGA microparticles: Experimental and mathematical modeling. Int J Pharm. 2018; 536: 360–369. https://doi.org/10.1016/j.ijpharm.2017.12.006 PMID: 29217474

119. Wang S, Suhaimi H, Mabrouk M, Das DB. Effects of Scaffold Pore Morphologies on Glucose Transport Limitations in Hollow Fibre Membrane Bioreactor for Bone Tissue Engineering: Experiments and Numerical Modelling. Membranes (Basel). 2021; 11. https://doi.org/10.3390/membranes11040257 PMID: 33918241

120. Paolino D, Tudose A, Celia C, Di Marzio L, Cilurzo F, Mircioiu C. Mathematical models as tools to predict the release kinetic of fluorescein from lyotropic colloidal liquid crystals. Materials (Basel). 2019; 12. https://doi.org/10.3390/ma12050693 PMID: 30813650

121. Siepmann J, Siepmann F. Mathematical modeling of drug delivery. Int J Pharm. 2008; 364: 328–343. https://doi.org/10.1016/j.ijpharm.2008.09.004 PMID: 18822362

122. Bar-Gera H. The Target Parameter of Adjusted R-Squared in Fixed-Design Experiments. Am Stat. 2017; 71: 112–119. https://doi.org/10.1080/00031305.2016.1200489

123. Yehia AF, Saleh M. An Adjusted Correlation Coefficient for Canonical Correlation Analysis. 2016.

124. Paarakh MP, Jose PANI, Setty CM, Peter G V. Release Kinetics—Concepts and Applications. Int J Pharm Res Technol. 2019; 8: 12–20. https://doi.org/10.31838/ijprt/08.01.02

125. Ratner B. The correlation coefficient: Its values range between 1/1, or do they. J Targeting, Meas Anal Mark. 2009; 17: 139–142. https://doi.org/10.1057/jt.2009.5

126. Mediavilla FAM, Landrum F, Shah V. A comparison of the coefficient of predictive power, the coefficient of determination and AIC for linear regression. J Appl Bus Econ. 2008; 1261–1266. Available from: http://www.digitalcommons.www.na-businesspress.com/JABE/MendezWeb.pdf

127. Gayawan E, Ipinyomi RA. A comparison of Akaike, Schwarz and R square criteria for model selection using some fertility models. Aust J Basic Appl Sci. 2009; 3: 3524–3530. Available from: http://www.ajbasweb.com/old/ajbas/2009/3524-3530.pdf

128. Yamaoka K, Nakagawa T, Uno T. Application of Akaike's information criterion (AIC) in the evaluation of linear pharmacokinetic equations. J Pharmacokinet Biopharm. 1978; 6: 165–175. https://doi.org/10.1007/BF01117450 PMID: 671222

129. Siepmann J, Peppas NA. Modeling of drug release from delivery systems based on hydroxypropyl methylcellulose (HPMC). Adv Drug Deliv Rev. 2001; 48: 139–157. https://doi.org/10.1016/s0169-409x(01)00112-0 PMID: 11369079

130. Zhao J, Wang L, Fan C, Yu K, Liu X, Zhao X, et al. Development of near zero-order release PLGA-based microspheres of a novel antipsychotic. Int J Pharm. 2017; 516: 32–38. https://doi.org/10.1016/j.ijpharm.2016.11.007 PMID: 27825865

131. Azadi S, Ashrafi H, Azadi A. Mathematical modeling of drug release from swellable polymeric nanoparticles. J Appl Pharm Sci. 2017; 7: 125–133. https://doi.org/10.7324/JAPS.2017.70418

132. Mulye N V., Turco SJ. A Simple Model Based on First Order Kinetics to Explain Release of Highly Water Soluble Drugs from Porous Dicalcium Phosphate Dihydrate Matrices. Drug Dev Ind Pharm. 1995; 21: 943–953. https://doi.org/10.3109/03639049509026658

133. Peppas N. Chemical and Physical Structure of Polymers as Carriers for Controlled Release of Bioactive Agents: A Review. J Macromol Sci Part C. 1983; 23: 61–126. https://doi.org/10.1080/07366578308079439

134. Vasconcelos A, Vega E, Pérez Y, Gómara MJ, García ML, Haro I. Conjugation of cell-penetrating peptides with poly(Lactic-co-glycolic acid)-polyethylene glycol nanoparticles improves ocular drug delivery. Int J Nanomedicine. 2015; 10: 609–631. https://doi.org/10.2147/IJN.S71198 PMID: 25670897

135. Papadopoulou V, Kosmidis K, Vlachou M, Macheras P. On the use of the Weibull function for the discernment of drug release mechanisms. Int J Pharm. 2006; 309: 44–50. https://doi.org/10.1016/j.ijpharm.2005.10.044 PMID: 16376033

136. Costa P, Manuel J, Lobo S. Modeling and comparison of dissolution profiles. Eur J Pharm Sci. 2001. Available from: www.elsevier.nl/locate/ejps PMID: 11297896

137. Barzegar-Jalali M, Adibkia K, Valizadeh H, Shadbad M, Nokhodchi A, Omidi Y, et al. Kinetic Analysis of Drug Release From Nanoparticles. J Pharm Pharm Sci. 2008; 11: 167–177. https://doi.org/10.18433/j3d59t PMID: 18471378

138. Ignacio M, Chubynsky M V., Slater GW. Interpreting the Weibull fitting parameters for diffusion-controlled release data. Phys A Stat Mech its Appl. 2017; 486: 486–496. https://doi.org/10.1016/j.physa.2017.05.033

139. Tomic I, Vidis-Millward A, Mueller-Zsigmondy M, Cardot JM. Setting accelerated dissolution test for PLGA microspheres containing peptide, investigation of critical parameters affecting drug release rate and mechanism. Int J Pharm. 2016; 505: 42–51. https://doi.org/10.1016/j.ijpharm.2016.03.048 PMID: 27025293

140. Kosmidis K, Argyrakis P, Macheras P. A reappraisal of drug release laws using Monte Carlo simulations: The prevalence of the Weibull function. Pharm Res. 2003; 20: 988–995. https://doi.org/10.1023/a:1024497920145 PMID: 12880283

141. Kobryń J, Sowa S, Gasztych M, Dryś A, Musiał W. Influence of hydrophilic polymers on the β factor in weibull equation applied to the release kinetics of a biologically active complex of aesculus hippocastanum. Int J Polym Sci. 2017; 2017. https://doi.org/10.1155/2017/3486384

142. Sitta DLA, Guilherme MR, da Silva EP, Valente AJM, Muniz EC, Rubira AF. Drug release mechanisms of chemically cross-linked albumin microparticles: Effect of the matrix erosion. Colloids Surfaces B Biointerfaces. 2014; 122: 404–413. https://doi.org/10.1016/j.colsurfb.2014.07.014 PMID: 25087021

143. Miles J. R Squared, Adjusted R Squared. Wiley StatsRef Stat Ref Online. 2014; 2–4. https://doi.org/10.1002/9781118445112.stat06627

144. Nandi AK. Model Order Selection from Noisy Polynomial Data without Using Any Polynomial Coefficients. IEEE Access. 2020; 8: 130417–130430. https://doi.org/10.1109/ACCESS.2020.3008527

145. Mohammed EA, Naugler C, Far BH. Emerging Business Intelligence Framework for a Clinical Laboratory Through Big Data Analytics. Emerging Trends in Computational Biology, Bioinformatics, and Systems Biology: Algorithms and Software Tools. Elsevier Inc.; 2015. https://doi.org/10.1016/B978-0-12-802508-6.00032-6

146. Jenkins DG, Quintana-Ascencio PF. A solution to minimum sample size for regressions. PLoS One. 2020; 15: e0229345. https://doi.org/10.1371/journal.pone.0229345 PMID: 32084211